STEEP SPATIAL CHEMICAL GRADIENTS IN SHALLOW GROUNDWATER CONTAMINATED WITH NITRATE AT A RESIDENTIAL SITE

By

CHRISTOPHER J. GEYER

Bachelor of Science in Geology

Oklahoma State University

Stillwater, Oklahoma

2011

Submitted to the Faculty of the
Graduate College of the
Oklahoma State University
in partial fulfillment of
the requirements for
the Degree of
MASTER OF SCIENCE
May, 2014

STEEP SPATIAL CHEMICAL GRADIENTS IN

SHALLOW GROUNDWATER CONTAMINATED

WITH NITRATE AT A RESIDENTIAL SITE

Thesis Approved:

Eliot Atekwana, PhD

Tracy Quan, PhD

Joseph Donoghue, PhD

ACKNOWLEDGMENTS

I thank Dr. Eliot Atekwana for the years spent patiently guiding my education and providing me with an opportunity to broaden not only my skill set, but also my world experience. Special gratitude is due to Dr. Wayne and Phyllis Pettyjohn, for the use of their property, their encouraging advice, and the many good times I had while in their company.

I thank my committee members Dr. Tracy Quan and Dr. Joseph Donoghue, who took time out of their busy schedules to help me, and provide their valuable insights into the writing process. I also wish to thank all the students who aided in collecting and processing of the samples- Eric Seeger, Nicole Paizis, Mary Niles, Eric Akoko, and the students of the Geochemistry classes from 2008, 2009, 2010, and 2011.

Acknowledgements reflect the views of the author and are not endorsed by committee members or Oklahoma State University.

Name: Christopher J. Geyer

Date of Degree: MAY, 2014

Title of Study: STEEP SPATIAL CHEMICAL GRADIENTS IN SHALLOW GROUNDWATER CONTAMINATED WITH NITRATE AT A RESIDENTIAL SITE

Major Field: Geology

Abstract: Shallow groundwater at a residential property in north-central Oklahoma was assessed to determine the extent of NO_3^- contamination and the effect of nitrate attenuation on groundwater chemistry. We hypothesized that denitrification at the site is the primary process controlling NO_3^- attenuation. The objectives of this investigation were to identify the potential sources and processes which control NO_3^- distributions, and observe the impact denitrification had on groundwater chemistry. Groundwater was sampled quarterly over a three-year period and analyzed for physical, chemical, and stable carbon isotopic composition. Persistent high concentrations of NO_3^- were observed with non-uniform distributions both temporally and spatially. The high persistence in NO_3^- contamination was attributed to upgradient application by residents, on-site application of fertilizers on flower beds and for lawn care, and contamination from a leaky sewer pipe. Variable NO_3^- concentrations were observed across the 40 m x 60 m site over a the study period. Temporal and spatial variations in NO_3^- concentrations were attributed to non-uniform fertilizer application, focused rain recharge with lower NO_3^- concentrations and denitrification. Nitrate concentrations were relatively low at a location suspected of effluent contamination, indicating NO_3^- attenuation at that location was accelerated. The stable carbon isotope ratios of dissolved inorganic carbon ($\delta^{13}C_{DIC}$) showed consistent depletion in groundwater at locations where it was suspected denitrification was fueled by organic matter. Marked increase in HCO_3^- and DIC and decreases in $\delta^{13}C_{DIC}$ suggests that weathering of carbonates coupled to organic matter mineralization by microbial activity was occurring in groundwater at the site.

TABLE OF CONTENTS

Chapter

LIST OF TABLES

Table Page

LIST OF FIGURES

Figure Page

CHAPTER I

INTRODUCTION

Human activities have exerted increasing influence on the nitrogen cycle at a global scale (Burow et al., 2010; Mastrocicco et al., 2011; Stuart et al., 2014). Anthropogenic influence of the global nitrogen cycle is primarily attributed to the widespread application of nitrogen bearing fertilizers, with up to 60% of the nitrogen lost as nitrate (NO_3^-) to groundwater (Burow et al., 2010; Canfield et al., 2010). Application of nitrogenous fertilizers has increased to more than ten times the amount applied in the 1950s (Robertson and Vitousek, 2009). Nitrate concentrations in many agricultural watersheds exceed the US EPA maximum contaminant level (MCL) of 10 mg/L of NO_3^- (Burow et al., 2010; US-EPA, 1976). The potential for increased leaching and runoff of fertilizers from agricultural fields will increase as demand for more food increases as the world's population increases (Trudell et al., 1986). Nitrate in drinking water was first recognized as a problem in the 1970s with health risks such as methahemoglobinemia, also known as "Blue Baby Syndrome" and multiple cancers attributed to ingestion of NO_3^- (Kite-Powell and Harding, 2006; Spalding and Exner, 1993; US-EPA, 1976). Among the environmental concerns regarding NO_3^- contamination of groundwater are the eutrophication of surface waters and significant changes to groundwater geochemistry and water-rock interactions (Böhlke, 2002; Rivett et al., 2008; Seitzinger, 2008).

Nitrate is rarely the primary form of nitrogen in fertilizers (Canfield et al., 2010; Kite-Powell and Harding, 2006; Nascimento et al., 1997; Stuart et al., 2014). The primary form of nitrogen in nitrogenous fertilizers is typically either ammonium (NH_4^+) or urea ($CO(NH_2)_2$) with urea as the dominant form of nitrogen in fertilizers applied at residential sites (Canfield et al., 2010; Ross, 1988). Bacteria capable of converting NH_4^+ and $CO(NH_2)_2$ to NO_3^- by nitrification carry out this process wherever NH_4^+ and $CO(NH_2)_2$ are available (Brunet et al., 2011; Kuenen and Robertson, 1994). Microbes can further degrade nitrogen with a reduction of NO_3^- to N_2O or N_2 by denitrification (Delwiche and Bryan, 1976; Knowles, 1982; Seitzinger et al., 2006). Denitrification rates are typically measured by using changes in the stable isotope of nitrogen ($\delta^{15}N$) or ratios of nitrogen species (NO_3^-, N_2O, N_2) supported by comparisons between NO_3^- and tracers such as Br^- or Cl^- (Aravena and Robertson, 1998; Green et al., 2010; Seitzinger et al., 2006; Trudell et al., 1986). Aspects of groundwater such as pH, ion concentrations, and carbonate speciation are significantly altered by denitrification (Böhlke, 2002; Brunet et al., 2011; Nascimento et al., 1997; Trudell et al., 1986).

Many investigations have been conducted with the goal of quantifying nitrification and denitrification rates whereas few have examined the potential effects nitrification and denitrification processes have on their environments other than eutrophication (Davidson et al., 1990; Green et al., 2010; Rivett et al., 2008; Seitzinger et al., 2006). Studies focused on the occurrence and fate of NO_3^- contamination in groundwater have been predominantly conducted in agricultural, rural, or riparian sites (Böhlke, 2002; Kite-Powell and Harding, 2006; Spalding and Exner, 1993; Trudell et al., 1986). Few investigations have been conducted on the occurrence and effect of NO_3^-

contamination on shallow groundwater in residential settings (Burow et al., 2010; Spalding and Exner, 1993). The prevailing assumption in many of these studies is that nitrification and denitrification are occurring within the groundwater and that they are essentially uniform across the study area investigated. New research has begun to identify locations or periods of time where denitrification is uniquely active within wetlands (Palta, 2012). Additionally, the effects of land use are assumed to be uniform across many study sites, which may not apply to small scale residential settings. Factors unique to residential environments such as roof runoff, and spot application of fertilizers may impact the spatial contamination and attenuation of NO_3^-. Compared to research in agricultural, rural and riparian settings, the fate of NO_3^- in groundwater in residential settings is largely unknown (Seitzinger et al., 2006). There is also a gap in knowledge concerning how land use practices specific to residential areas influence NO_3^- contamination. To gain greater insights into anthropogenic influence on the nitrogen cycle, the occurrence and influence of NO_3^- within residential properties must be studied.

Here we report on a study in which we investigated the spatial and temporal NO_3^- distributions, as well as the effect of NO_3^- attenuation on groundwater chemistry in a shallow residential aquifer. The site has been previously studied for hydrology and groundwater quality (Hagen, 1986; Hoyle, 1989; Ross, 1988). Previous studies have determined the the source of calcium in groundwater is likely from calcite nodules in the soil (Ross, 1988). Background NO_3^- concentrations in groundwater across the United States are typically estimated to be below 1 mg/L while NO_3^- concentrations measured in groundwater at this site since 1986 were above the US EPA MCL (Hagen, 1986; Panno et al., 2006). The persistent NO_3^- concentration above US EPA MCL within the

groundwater makes this study site an ideal location to identify potential sources and sinks of NO_3^-, as well as to determine the effects of NO_3^- attenuation on groundwater chemistry.

We hypothesize that NO_3^- attenuation is occurring in groundwater at the site and that this attenuation is via denitrification. Additionally we hypothesize that denitrification alters the chemistry of the groundwater. The objectives of this study were to (1) identify the source(s) of NO_3^-; (2) identify the processes which control NO_3^- distributions; and (3) identify rock-water interactions within the shallow aquifer that are linked to denitrification. In order to accomplish the objectives of this study, chemical and isotopic parameters that could be influenced by the presence of and attenuation of NO_3^- were examined over space and time. The parameters investigated include concentration of NO_3^- and other major ions, pH, water level, and the stable carbon isotopes of dissolved inorganic carbon ($\delta^{13}C_{DIC}$).

CHAPTER II

THEORETICAL OVERVIEW

2.1 Potential sources of NO_3^- contamination

The location of this study contains four potential sources for NO_3^- contamination. One potential source is a sewer line which runs north to south along the western border of the property and a second potential source is another sewer line which runs west to east along the southern border of the property (Fig. 1). Fertilizers applied to properties upgradient of the study site and applied at the site make up the third and fourth potential sources of NO_3^- contamination. Nitrate contamination from sewage is usually accompanied by an influx of organic matter and Cl^- concentrations above background concentrations in groundwater (Aravena and Robertson, 1998). Groundwater depth plays an important role in NO_3^- contamination as the depth of the sewer lines is 2.4 m. When the groundwater level is below the sewer lines, any break in the piping will result in contamination of groundwater. If NO_3^- contamination was only because of the application of fertilizers on properties upgradient of the study site, we would expect that the NO_3^- concentration of upgradient groundwater will be above the 1 mg/L considered background. Additionally, if there is no on-site NO_3^- contamination, concentrations of NO_3^- in groundwater that flows through the site will remain unchanged or decrease because of attenuation. Since fertilizer applied to flower beds on site is designed for slow release, it is unlikely that individual pulses correlating to single applications would be

evident especially considering the frequency of sampling in this study. If application of fertilizers to grass for lawn care is the primary source of NO_3^- contamination a homogenous distribution of NO_3^- would be observable in the groundwater across the study site. Owners of residences in the neighborhood where this study was conducted apply fertilizers up to five times a year to achieve "socially acceptable lawns" (Hagen, 1986). Application of fertilizers typically on-site occurs in April, May, June, August, and November (Pettyjohn, personal communication).

2.2 Hydrogeological considerations

The spatial distributions of NO_3^- will in part be controlled by the direction of groundwater flow. During periods where the water table is above 2.2 m, groundwater flows south-west toward an unnamed intermittent stream. During periods where the water table is below 2.2 m groundwater flow direction is south and discharges into a storm drain channel south of the property (Pettyjohn, 1989b). Also, within the residential setting, recharge of groundwater is influenced by irrigation activities, thus groundwater depth may reflect recharge from precipitation and irrigation applications.

2.3 Chemical evolution of NO_3^-

There are two main processes that have been identified as the primary controls on nitrogen attenuation within groundwater- nitrification and denitrification (Delwiche and Bryan, 1976; Knowles, 1982; Palta, 2012; Seitzinger et al., 2006). The combined products of these reactions may have significant effects on groundwater chemistry.

2.3.1 Nitrification

Nitrification is a microbially driven process whereby NH_4^+ and other nitrogen species are converted into NO_3^-. Fertilizers used for plant growth commonly contain nitrogen in the form of urea, although other forms such as ammonia (NH_3) and ammonium nitrate (NH_4NO_3) are not uncommon (Böhlke, 2002). Urea is the dominant form of nitrogen in the fertilizers applied at the study site and surrounding residences (Ross, 1988). Urea, ammonium, and ammonia either from fertilizer or effluent, undergo reactions which convert the nitrogen to a more labile form. After the application of ammonia and urea bearing fertilizers, hydrolysis of the urea produces ammonia (Eqn. 1).

$$NH_2CONH_2 + H_2O \leftrightarrow CO_2 + 2NH_3 \quad (1)$$

The oxidation of ammonia (Eqn. 2) followed by conversion of NO_2^- to NO_3^- (Eqn. 3), both performed by microorganisms is commonly referred to as nitrification (Ward et al., 2011).

$$2NH_3 + 3O_2 \leftrightarrow 2NO_2^- + 2H^+ + 2H_2O \quad (2)$$

$$NO_2^- + H_2O \leftrightarrow NO_3^- + 2H^+ \quad (3)$$

If nitrification is occurring in groundwater upgradient and across the site, NO_3^- concentrations above background (1 mg/L) would be expected. If NO_3^- attenuation is not denitrification, but instead a lack of nitrification, consistent low NO_3^- concentrations would be observable as groundwater enters and travels across the site.

2.3.2 Denitrification

Denitrification occurs from microbial conversion of NO_3^- to N_2O or N_2. This conversion requires an electron donor such as organic carbon (Eqn. 4) and is considered the primary mechanisim for NO_3^- loss within aquifers (Böhlke, 2002; Rivett et al., 2008;

Knowles, 1982; Nascimento et al., 1997). The availability of organic carbon is one of the most important limiting factors controlling the activity of denitrifying bacteria (Delwiche and Bryan, 1976; Knowles, 1982)

$$5C + 4NO_3^- + 4H^+ \leftrightarrow 2N_2 + 5CO_{2(aq)} + 2H_2O \quad (4)$$

It was considered in the past that denitrification could not compete with oxygen reduction and that denitrification could only occur in anaerobic conditions in groundwater (Delwiche and Bryan, 1976). However as research on denitrification has progressed, it has been recognized that denitrification occurs not only in anaerobic, but aerobic environments as well (Delwiche and Bryan, 1976; Knowles, 1982; Lloyd, 1993). Explanations for the occurrence of denitrification under aerobic conditions commonly cite two plausible situations: (1) the existence of bacteria capable of denitrification in an environment with excess oxygen, or (2) the existence of micro-sites where anoxic conditions exist and are not represented by the larger water body (Kuenen and Robertson, 1994; Rivett et al., 2008).

The rates of nitrification or denitrification were not measured in this study. However, if denitrification is taking place several outcomes are possible. First, if NO_3^- sources are solely from upgradient contamination NO_3^- concentrations will be above background and exhibit a consistent decrease as groundwater travels downgradient. If denitrification is heterogeneous accross the site, the products of denitrification, such as CO_2, will be elevated at locations where denitrification is active. Additionally the stable isotopes of dissolved inorganic carbon ($\delta^{13}C_{DIC}$) will be depleted as organic carbon is consumed by denitrification is converted to CO_2 that enters the groundwater DIC pool.

2.3.3 Products and reactions from NO_3^- evolution

During denitrification, there is concurrent utilization of organic carbon (C_{org}) and H^+. The H^+ produced during nitrification (Eqn. 3) and consumed during denitrification (Eqn. 4) causes the pH to decrease and increase, respectively. While rates of denitrification are usually positively related to pH, the process of nitrification or denitrification cannot be quantified by the change in pH alone, since potential decreases in pH may be buffered by the production of HCO_3^- from carbonate dissolution (Eqn. 5 and 6) and other reactions during carbonate evolution (Eqn. 7 and 8) (Böhlke, 2002; Drever, 1997; Hounslow, 1995).

$$H^+ + CaCO_3 \leftrightarrow Ca^{2+} + HCO_3^- \quad (5)$$

$$CO_{2(aq)} + CaCO_3 + H_2O \leftrightarrow Ca^{2+} + 2\ HCO_3^- \quad (6)$$

$$CO_{2(g)} \leftrightarrow H_2O + CO_{2(aq)} \leftrightarrow H_2CO_3^- \quad (7)$$

$$HCO_3^- + H^+ \leftrightarrow H_2CO_3^- \quad (8)$$

One of the by-products of nitrification and denitrification is $CO_{2(aq)}$ which can affect the partial pressure of $CO_{2(g)}$ (pCO_2) concentrations in groundwater (Eqn. 1 and 4). The $CO_{2(aq)}$ can dissociate to H_2CO_3 or degas, thereby increasing the pCO_2 (Eqn. 7). If the products of denitrification and nitrification enhance carbonate weathering, a relationship should be observable between the products of the denitrification and carbonate dissolution. Elevated pCO_2 caused by nitrification and denitrification, in conjunction with high HCO_3^-, DIC, and Ca^{2+} concentrations can thus be used as evidence that processes such as nitrification and denitrification may be the driving mechanisms for carbonate weathering within aquifer (Ali and Atekwana, 2011; Langmuir, 1971).

CHAPTER III

METHODOLOGY

3.1 Site Description

The study site is a residential property located in Payne County in north-central Oklahoma (36˚8'16" N, 97˚3'16" W) (Fig. 1). The property is situated in the Boomer Creek floodplain, underlain by approximately 15.2 m of Quaternary alluvium filling a valley formed in the Upper Pennsylvanian Doyle Shale. The alluvium is comprised of intermixed sand (50%), silt (25%), and clay (25%) (Hoyle, 1989; Pettyjohn, 1989a). The topography at the site exhibits little relief (<25 cm) with a slope of 1%. The soil is an Ashport type that is formed in loamy alluvium of Holocene age and associated with good drainage because of the presence of macro-pores (Pettyjohn, 1989a; Ross, 1988). The transmissivity and hydraulic conductivity of the shallow aquifer average 27.6 m^2 d^{-1} and 2 m d^{-1}, respectively (Hagen, 1986; Pettyjohn, 1989a; Ross, 1988).

The study area has a temperate climate and is considered semi-arid. The average ambient air temperatures range from 27.5˚C in the summer to 0.88˚C in the winter, with annual precipitation averaging 826.7±283 mm for 2008 to 2011 (Fedstats, 9-2-2013; Mesonet, 2014). Precipitation generally occurs between the months of March and June as short, high intensity showers. The shallow groundwater is recharged by precipitation and

lawn irrigation. Groundwater generally flows to the south-south west (Fig. 1)(Pettyjohn, 1989b).

3.2 Water Sampling

Groundwater was sampled from monitoring wells (MW) quarterly beginning in September 2008 until October 2011. The monitoring wells are constructed of 5-cm diameter PVC pipe that are screened and sand packed. The annular space is filled with bentonite (Pettyjohn, 1989a). Monitoring wells G, H, B, A, E, C and D (Fig. 1) are 4.2 m deep and screened along the lower 1.8 m. Monitoring well F is 12.2 m deep and is screened along the lower 9.1 m.

3.3 Sampling and Analysis

Prior to sampling, water table depth was recorded using a Solinst electronic water level meter. Groundwater was pumped to the surface using a peristaltic pump through a flow cell into which a Yellow Springs Instruments (YSI) multi-parameter probe was immersed. The temperature and specific conductance were monitored and after the readings were stable, physical parameters were recorded and water was collected for chemical and isotopic measurements. The temperature, pH, oxidation-reduction potential (ORP), dissolved oxygen (DO), specific conductance, and total dissolved solids (TDS) were measured in the flow cell using a YSI multi-parameter probe, calibrated to the manufacturers' specifications. After measuring the physical parameters, samples collected for chemical were filtered through 0.45 µM filters and collected in 30 mL high-density polyethylene (HDPE) bottles for anions and in pre-acidified (high-purity HNO_3) 60 mL HDPE bottles for cations. Water for measurement of dissolved inorganic carbon (DIC) and stable carbon isotopes of DIC ($\delta^{13}C_{DIC}$) were were filtered through 0.45 µM

filters and collected in pre-acidified (1 mL of 85% H_3PO_4) vacutainer tubes (Atekwana and Krishnamurthy, 1998).

Alkalinity was measured during sampling by titration with sulfuric acid using a Hach digital titrator (Hach, 2013). Anions (Cl^-, SO_4^{2-} and NO_3^-) were measured using a Dionex Ion Chromatography System (ICS 3000). Cations (Ca^{2+}, Mg^{2+}, Na^+ and K^+) were measured using the Dionex Ion Chromatography System (ICS 3000) or a Perkin Elmer Inductively Coupled Plasma Optical Emissions Spectrometer (Optima 2100 DV). Analyses of ions on either the ICS 3000 or Optima 2100 DV were obtained with a precision of better than 2% on replicated measurements of standards and duplicate samples. $CO_{2(g)}$ for stable carbon isotopic measurement of DIC was extracted from the vacutainers tubes as described by Atekwana and Krishnamurthy (1998). Concentrations of DIC were calculated from the extracted $CO_{2(g)}$, sealed in Pyrex tubes and subsequently analyzed for $\delta^{13}C$ using a Thermo Finnegan Delta Plus XL isotope ratio mass spectrometer. DIC values were measured using a pressure transducer with a precision of better than 1%. Carbon isotopes are reported in delta (δ) notation in per mil (‰):

$$\delta(‰)=\left(\left(\frac{R_{sample}}{R_{std}}\right)-1\right)x\ 1000$$

Where R is the ratio $^{13}C/^{12}C$, R_{sample} is the ratio of $^{13}C/^{12}C$ in the sample and R_{std} is the ratio of $^{13}C/^{12}C$ in the standard. The $\delta^{13}C$ values are reported relative to Vienna Pee Dee Belemnite (VPDB). Samples and routine precision checks using in-house carbonate standards yield an overall precision of ±0.1‰ or better.

3.4 Geochemical Modeling

The partial pressure of $CO_{2\ (aq)}$ (log pCO_2) in the samples was modeled with PHREEQC version 2.18 using corresponding pH, DIC concentration, and temperature

(Parkhurst, 1995). The saturation index with respect to calcite (SI_{cal}) was calculated with PHREEQC using corresponding pH, alkalinity, Ca^{2+}concentration, and temperature (Parkhurst, 1995).

3.5 Statistical Analysis

Descriptive statistics and correlation coefficients (R) were calculated using the data analysis package in Microsoft Excel 2013. Statistical analyses were performed with a level of significance of p=0.05. The coefficient of variation (expressed as a percentage), also known as the relative standard deviation (RSD) was calculated using averages and standard deviations (Schot and Pieber, 2012). The RSD was used to assess the variation of individual parameters in each monitoring well over the entire course of this study (RSD-t). The spatial relative standard deviation (RSD-s) of an individual parameter was calculated for all sampling locations using values from all sampling events.

CHAPTER IV

RESULTS

Descriptive statistics of the chemical, physical, and isotopic measurements for groundwater at the study site are listed in Table 1. The correlation coefficients of the chemical, physical, and isotopic data are listed in Table 2. The complete results are presented in supplementary Table S1.

4.1 Water Level and Temperature

Groundwater depth averaged 2.9±0.5 m and varied between 1.2 to 3.8 m (Table 1). Groundwater temperatures average 18.5±3.2 °C and varied between 12.5 and 27.5 °C (Table 1). Variations in groundwater level and temperature across the site are plotted in Fig. 2. High water periods were observed in the spring seasons, these periods are indicated by shading in Fig. 2a. High water periods do not directly reflect recharge from only rain water because the recharge of this shallow aquifer can be significantly impacted by antecedent moisture conditions (Ross, 1988). Artificial recharge because of irrigation systems may also be responsible for elevated groundwater, as high periods in water table depth correspond to growing seasons. Groundwater temperatures begin to increase towards the end of February and the beginning of March and then begin to decrease in November. High periods in groundwater level precede high periods in groundwater temperature, this is expected because of summer and winter seasonality. Increased precipitation is observed in the spring season.

4.2 Nitrate Concentrations

NO_3^- concentrations in groundwater average 36.8±37.0 mg/L and range from 0.1 to 214.0 mg/L (Table 1). As groundwater flows to the study site (Fig. 1), NO_3^- concentrations in groundwater at MW-G and MW-H average 57.7±18.3 mg/L and 47.6±11.0 mg/L, respectively. As groundwater travels through the study site, NO_3^- concentrations increase at MW-A to an average of 77.8±38.4 mg/L, decrease at MW-B to 7.0±3.5 mg/L, at MW-E to 4.8±3.3 mg/L, and at MW-F to 20.5±11.3 mg/L. Before leaving the site, groundwater in the south west downgradient area at MW-C has average NO_3^- concentrations of 66.8±48.9 mg/L whereas in the south eastern downgradient area at MW-D, the average concentration of NO_3^- is 4.6±2.8 mg/L.

Temporal variations of the nitrate concentrations across the site are shown in Fig. 3. Temporal variations are apparent for most monitoring well locations with alternating periods of high and low NO_3^- concentrations observable in MW-G, MW-B, MW-E, MW-A, MW-F. The periodic increases or decreases in NO_3^- concentrations occurred during high groundwater for some locations and during low groundwater levels for others (Fig. 3). Overall, temporal decrease in NO_3^- was observed in groundwater at MW-H and MW-C, whereas other locations such as MW-G and MW-A showed persistently high concentrations throughout the study (Fig. 3).

4.3. pH, alkalinity, DIC and $\delta^{13}C_{DIC}$

Groundwater pH across the site varied from 4.5 to 7.4 and averaged 6.4±.6 (Table 1). The pH of groundwater entering the site at MW-G and MW-H averaged 6.5±0.4 and 6.8±0.4, respectively. As groundwater traveled through the study site, average pH remained relatively unchanged with values of 6.3±0.3 at MW-A, 5.9±0.9 at MW-B,

6.5±0.7 at MW-E, and 6.3±0.6 at MW-F. Before leaving the site, the average groundwater pH in the south west downgradient MW-C was 6.5±0.4, whereas in the south eastern downgradient area at MW-D was 6.7±0.3 (Table. 1).

HCO_3^- concentrations averaged 375±177 mg/L and ranged between 48 and 793 mg/L(Table 1). HCO_3^- concentrations for groundwater entering the site averaged 448.1±25.2 mg/L for MW-G and 454.7±36.9 mg/L for MW-H. Midgradient monitoring wells had lower HCO_3^- averaging 94.8±32.9 mg/L for MW-B, 133.6±24.1 mg/L for MW-E, 404.8±30.1 mg/L for MW-A, and 336.1±121.4 mg/L for MW-F. As groundwater leaves the study site, average HCO_3^- concentrations for MW-C were 490.2±121.8 mg/L and 605.4±61.9 mg/L for MW-D (Table 1). Midgradient, groundwater at MW-B and MW-E show relatively low HCO_3^-, while locations MW-F and MW-A had HCO_3^- concentrations slightly lower than upgradient (Fig. 4). Groundwater at the south eastern downgradient location MW-D exhibited the highest HCO_3^- concentrations at the site, whereas the south western location MW-C had HCO_3^- concentrations only slightly higher than the initial groundwater entering the site (Fig. 4). Over time, groundwater at MW-G and MW-H show little variation in HCO_3^- concentration while MW- B, MW-E, MW-A, and MW-F show periodic increasing and decreasing HCO_3^- concentrations (Fig. 4). Groundwater exiting the study site at MW-C and MW-D show much higher HCO_3^- concentrations but with much more variability than groundwater upgradient. HCO_3^- distribution was not uniform across the site and can be described as generally increasing downgradient except for MW-B and MW-E, which are midgradient at the site (Fig. 4).

Dissolved inorganic carbon (DIC) concentrations ranged from 3.1 to 171.9 mg C/L. As groundwater entered the site, DIC concentrations were 87.0±14.6 mg C/L for

MW-G and 85.7±11.3 mg C/L for MW-H. Groundwater midgradient at the site, MW-B, MW-E, MW-A, and MW-F, had DIC concentrations of 19.4±6.8, 28.0±36.2, 79.3±14.6 and 69.7±18.0 mg C/L, respectively. Groundwater in the downgradient locations had DIC concentrations of 100.8±34.9 mg C/L for MW-C and 120.4±20.1 mg C/L for MW-D. Groundwater decreased in DIC concentrations midgradient relative to upgradient monitoring wells, then increased to above the initial DIC concentrations as groundwater leaves the site (Table 1).Temporal fluctuations in dissolved inorganic carbon (DIC) for each of the sampling locations have been shown in Fig. 5. Except for MW-B and MW-E, which both remain relatively constant, DIC concentrations generally decrease over time (Fig 6).

Values for the $\delta^{13}C_{DIC}$ in groundwater averaged -11.9±2.5 ‰ and ranged from -16.2‰ to -7.4 ‰ (Table 1). As groundwater enters the site at MW-G and MW-H, the $\delta^{13}C_{DIC}$ values averaged -8.5±1.1 ‰ for MW-G and -8.3±0.4 ‰ for MW-H. By the middle of the site, sampling locations separate into two groups: MW-A and MW-F have average $\delta^{13}C_{DIC}$ values of -11.5±0.5 ‰ and -11.4±1.8 ‰, respectively, whereas MW-B and MW-E have values of -14.6±1.1 ‰ and -14.5±1.0 ‰, respectively. Monitoring well-D and MW-C were depleted in $\delta^{13}C_{DIC}$ with respect to the upgradient monitoring wells, with averages of -12.8±0.7 ‰ and -13.7±1.6 ‰, respectively. Temporal variations of $\delta^{13}C_{DIC}$ for each of the sampling locations are shown in Fig 7. Over time, the upgradient locations MW-G and MW-H, and midgradient monitoring wells A, B, E, and F remained nearly constant (Fig. 6). Groundwater from the south western downgradient location at MW-C exhibited a $\delta^{13}C_{DIC}$ depletion with periods of enrichment and depletion, whereas

MW-D is the only monitoring well to show a persistent depletion of $\delta^{13}C_{DIC}$ overtime (Fig. 6).

4.4. Major anions and cations

Dominant ions in the groundwater across the site are listed in order of abundance: $Ca^{2+} > Na^{+} > Mg^{2+} > K^{+}$ and $HCO_3^{-} > NO_3^{-} > Cl^{-} > SO_4^{2-}$ (Table 1 and S1). The cation and anion proportions are plotted on Fig. 7. The predominant water type at the site was Ca^{2+}-Mg^{2+}-HCO_3^{-}. However, groundwater at MW-F shows variation from Ca^{2+} to Na^{+}, MW-E shows variation from Ca^{2+} to Mg^{2+} and at MW-D the change is from Ca^{2+} to Mg^{2+} and HCO_3^{-} to Cl^{-}.

CHAPTER V

DISCUSSION

To understand the fate of NO_3^- and the chemical evolution of groundwater at this site, we evaluated the sources of NO_3^- contamination, the processes that attenuate NO_3^- in groundwater and the consequences of nitrate attenuation on groundwater geochemistry. Nitrate concentrations in some groundwater locations (MW-G, MW-H, MW-A, MW-F, MW-C) were persistently above the US EPA MCL of 10.0 mg/L (US-EPA, 1976) (Table S1). Although the study site is only 60 m x 40 m, the NO_3^- concentrations are spatially variable and show steep gradients (Fig. 9). Nitrate concentrations for all groundwater sampling locations show dissimilar temporal variability (Fig. 3). Moreover, the differences in the spatial and temporal behavior suggest multiple sources and processes that control NO_3^- concentrations in the shallow groundwater.

5.1 Sources of nitrate

One of the objectives of this study was to identify the potential sources for NO_3^- contamination. The results indicate that multiple sources are responsible for NO_3^- contamination at the site. A previous study at this site by Hagen (1986) recorded NO_3^- concentrations that averaged 6.0 ± 4.6 mg/L and ranged between 0.3 to 27.9 mg/L at MW-A (Fig. 1) over a nine month period. Compared to the present study, average NO_3^- concentrations in groundwater at MW-A have increased up to thirteen times the previous average reported by Hagen (1986) (Table 1).

One potential source of NO_3^- is from application and subsequent nitrification of fertilizers at upgradient properties in the neighborhood. As seen in Figure 3, groundwater entering the site at upgradient lcoations MW-G and MW-H are consistently above background concentrations, indicating NO_3^- contamination from upgradient sources. If the sole source of NO_3^- in groundwater were only from contamination upgradient at the study site, there would be a constant concentration or a general decrease in NO_3^- concentrations because of attenuation over the course of this study and no NO_3^- contamination occurring on-site. If NO_3^- contamination is because of periodic on-site applications of fertilizer, specific locations will exhibit periodic pulses of greater magnitude than other locations. Figure 3 shows temporal trends in NO_3^- concentrations. What can be observed in Figure 3 is that the midgradient locations MW-B, MW-E, MW-A and MW-F all exhibit periodic pulses in NO_3^- concentrations. Upgradient locations MW-G and MW-H show some variability in NO_3^- concentrations, but not consistent pulses that could be associated with seasonality (Fig. 3). Likewise, locations MW-C and MW-D show periodic pulses of NO_3^- which are asynchronous with seasonality (Fig. 3). Figure 10 shows the statistical summary of NO_3^- concentrations across the site. What can be observed in Figure 9 is that NO_3^- does not uniformly decrease downgradient of MW-H and MW-G even though initial upgradient concentrations at MW-G and MW-H exhibit higher than natural concentrations (Kite-Powell and Harding, 2006). On-site fertilizer application would result in increased NO_3^- concentrations downgradient, while decreased NO_3^- concentrations would indicate processes controlling NO_3^- attenuation exceed NO_3^- contamination. The average NO_3^- concentrations increase from upgradient to midgradient locations (e.g. MW-A; Fig. 9) which indicate NO_3^- contamination from fertilizers applied

to flowerbeds or as lawn care. Average NO_3^- concentrations then decrease from midgradient to downgradient locations (e.g. MW-D), indicating NO_3^- attenuation (Fig. 9). Considering that the concentrations of NO_3^- have been consistently high in most groundwater locations for the three year duration of the study and given the groundwater flow rate of 0.3 m/day, it is unlikely that the high NO_3^- concentrations observed in the groundwater are the results of a single contamination pulse (Ross, 1988).

In addition to fertilizer application, Ross (1988) has suggested that there is contamination of groundwater from a leaky sewer line which runs along the southern and western edges of the property (Fig. 1). Nitrate contamination from sewage is accompanied by Cl^- concentrations above background (Aravena and Robertson, 1998). The average concentration of Cl^- at MW-D is 145±48 mg/L compared to upgradient MW-G and H at 29±10 and 20±5 mg/L, respectively. The relationship between Cl^- and Na^+ shown in Fig. 10a can be used to argue that the Cl^- concentrations at MW-D are much higher relative to the other sampling locations. The same conclusion can also be obtained from the cation and anion proportions shown in Figure 7. If high concentrations of Cl^- were the result of winter application of road salt, all locations would likely exhibit periodically elevated Cl^- concentrations. Additionally, if the source of Cl^- were common salt, the ratio of Cl^-/Na^+ would be 1:1; which, as can be observed in Fig. 10a is not the case. Using Cl^- as an indicator for groundwater contamination by sewage, it can be demonstrated that only location MW-D has the potential for NO_3^- contamination from sewage. Moreover, no salts were applied on the property and on roads in the winter for de-icing during the period of study. Persistently high Cl^- concentrations in the absence of salt application is likely from a leaking sewer line. Effluent contamination is usually

observed in conjunction with nitrate contamination; the relatively low concentrations of NO_3^- suggest that NO_3^- attenuation at location D is particularly active.

5.2. Nitrate attenuation in groundwater

The second objective of this study was to identify the processes responsible for NO_3^- attenuation in groundwater. Nitrate attenuation can occur because of dilution from rainwater runoff or from denitrification.

5.2.1. Dilution

Previous studies have suggested that NO_3^- concentrations are significantly influenced by dilution if individual rain events are not preceded by surficial addition of nitrogen (Hagen, 1986; Ross, 1988). Monitoring well-B, MW-F, MW-E, and MW-D exhibit groundwater NO_3^- concentrations that are lower than the upgradient locations (Fig. 9). Monitoring well-B, MW-E and MW-D are located within small (2 m x 1 m) flower beds whereas MW-F is below a concrete driveway extending 2 m in all directions (Fig. 1). No chemical process capable of removing Cl^- has been identified at the study site, hence Cl^- can be used as an indicator of the process of dilution, with the exception of locations which are affected by sewage contamination (Goodale et al., 2009; Lovett et al., 2005). While Cl^- generally increases as groundwater travels through the study site, MW-B and MW-E exhibit Cl^- concentrations nearly one tenth the average concentrations of groundwater in upgradient locations at MW-G and MW-H, with a similar dilution ratio observed in NO_3^- concentrations. Since Cl^- is found in lower concentrations at MW-B and MW-E, it is reasonable to conclude the geochemistry of groundwater at these locations may be affected by dilution. Therefore we can conclude low concentrations of NO_3^- and other chemical constituents at MW-B and MW-E may be caused in part by dilution.

Dilution is likely explained by way of rain discharge from roof drain downspouts within 0.5 m of the each sampling locations. During rain events, rainwater runoff from the roof is channeled to the areas immediately around the downspouts, causing the surface in approximately a 1 m radius surrounding the downspouts to become flooded (Pettyjohn, 1989a). The chemical contribution from rainwater to the ion concentrations at MW-B and MW-E is minimal, but will result in much lower average ion concentrations (Table 1, Table S1).

5.2.2. Denitrification

In order to confirm denitrification as a means of NO_3^- attenuation, the products of denitrification were monitored. From equations 4, 7, and 8, pCO_2 and subsequently HCO_3^- can be shown to be products related to denitrification. $CO_{2(g)}$ may also be generated from oxidation of organic matter (Eqn. 9) involving no reduction in NO_3^- concentrations in groundwater.

$$CH_2O + O_2 \leftrightarrow CO_2 + H_2O \quad (9)$$

Since Table 1 shows that spatial distributions of DO are relatively uniform, we can conclude that no unique conditions promoting or inhibiting oxidation of organic matter exist at specific locations. Thus, it follows that if oxidation of organic matter is responsible for increased carbon concentrations in groundwater, dissolved inorganic carbon (DIC) content would be uniform throughout the site. However, based on Figure 5, it can be observed that the DIC concentration in groundwater exhibits steep gradients between sampling locations. Additionally fractionation of $\delta^{13}C_{DIC}$ will occur if oxidation of organic matter is microbially mediated, such as denitrification; Figure 6 displays $\delta^{13}C_{DIC}$ values which are relatively enriched at upgradient locations and relatively

depleted at downgradient locations. $\delta^{13}C_{DIC}$ fractionation will be discussed in more detail in section 6.3. With oxidation of organic carbon eliminated as a possibility for controlling CO_2 and NO_3^- concentrations, denitrification is the most likely process which can adequately describe the evolution of NO_3^- attenuation in groundwater.

Logically, $CO_{2(g)}$ produced during denitrification will adjust the equilibrium between $CO_{2(aq)}$ and HCO_3^-, thus as denitrification occurs, the pCO_2 and concentrations of HCO_3^- will increase concurrently. Groundwater log pCO_2 averaged $10^{-2.0\pm0.4}$ atm, with a range from $10^{-3.38}$ to $10^{-1.46}$ atm. Covariance of pCO_2 and HCO_3^- concentrations can be demonstrated by a positive correlation coefficient (R) of 0.55. If the absolute value of R lies between 0.5 and 0.69, sample sets are considered to have moderately strong correlation (Asuero et al., 2006; Schot and Pieber, 2012). If nitrification, and denitrification were occurring in an isolated system, it would be expected that the correlation coefficient would be near perfect ($R \geq 0.90$). However, natural groundwater such as in this study is subject to a myriad of other processes which interact with inorganic carbon species. Hence it would be highly unlikely that a near perfect correlation coefficient could be achieved when monitoring pCO_2 and other chemical parameters in natural groundwater. A positive correlation between pCO_2 and HCO_3^- concentration demonstrates that HCO_3^- in groundwater is related to the processes increasing the pCO_2 such as denitrification. Higher concentrations of HCO_3^- were observed in downgradient locations (e.g. MW-C, MW-D) compared to upgradient locations MW-G and MW-H, indicating denitrification does occur as groundwater travels through the site (Fig. 4). Likewise, if denitrification is responsible for carbonate dissolution, a correlation will exist between the products of the two processes. A

moderately strong correlation is observed between pCO_2 and Ca^{2+} with a correlation coefficient of 0.51 (Table S2)(Asuero et al., 2006; Langmuir, 1971). Thus, pCO_2, HCO_3^-, and Ca^{2+} concentrations can be used as proxy indicators of denitrification within aquifers containing carbonates.

As observed in Figure 3, there are periodic increases and decreases in NO_3^- concentrations. However, concentrations of NO_3^- are persistently high at MW-G, MW-H, MW-A and MW-C. One way to explain this is the periodic application of NO_3^- in excess of amounts consumed by denitrification. A constant supply of NO_3^- across the site is unlikely since fertilizers are applied periodically. Another way to explain consistent elevated NO_3^- concentrations is that the processes which attenuate NO_3^- are limited. Denitrification is commonly thought to be limited by availability of organic carbon and prevailing oxygen concentrations in groundwater. High concentrations of dissolved oxygen (DO) in groundwater were thought to inhibit denitrification (Delwiche and Bryan, 1976). However, recent studies have suggested denitrification in groundwater can occur when DO is present in concentrations above 0.5 mg/L (Lloyd, 1993). Denitrification has been observed in DO concentrations of up to 4.0 mg/L, albeit at decreasing rates as DO concentrations increase (Rivett et al., 2008). Dissolved oxygen concentrations in groundwater at the study site average 3.3±1.9 mg/L. If DO were the limiting factor controlling denitrification, locations with high DO concentrations would exhibit similarly elevated NO_3^- concentrations, whereas locations with lower DO content would have lower NO_3^- concentrations. If locations MW-G and MW-D are compared, both have similar average DO content (3.4±2.8 mg/L and 3.5±1.9 mg/L, respectively), however, MW-G has over ten times the average NO_3^- concentration compared to MW-D

(57.7±18.3 mg/L and 4.7±2.8 mg/L, respectively) (Table 1).Thus, it is unlikely that dissolved oxygen limits denitrification from occurring within the groundwater.

Many studies have noted that denitrification is highly dependent on the availability of labile organic carbon (Delwiche and Bryan, 1976; Knowles, 1982; Lofton et al., 2007; Mastrocicco et al., 2011; Rivett et al., 2008). It is thus reasonable to assume that denitrification rates are limited in many cases by organic carbon availabile to the bacteria. Such may be the case in this study, where persistently high concentrations of NO_3^- are observed upgradient at MW-G and MW-H, while MW-D shows uncharacteristically low concentrations of NO_3^- (Fig. 9). As groundwater travels downgradient, additional influx of NO_3^- because of application of fertilizers across the site is likely to increase groundwater NO_3^- concentrations. This can be observed when comparing groundwater at MW-G, MW-A, and MW-C (Fig. 3). Monitoring well C has high NO_3^- but also high HCO_3^- and Ca^{2+} concentrations compared to MW-G, and MW-H. Downgradient MW-C has lower concentrations of NO_3^- compared to the midgradient location MW-A which demonstrates that some NO_3^- attenuation occurs but does not with all available NO_3^-. However, MW-D is farthest downgradient and subject to no obvious sources of dilution, yet exhibits the lowest concentration range of NO_3^- of groundwater at the site (Fig. 9). For such complete attenuation of NO_3^- to occur at MW-D, this location must be subject to unique conditions augmenting denitrification. The almost complete attenuation of NO_3^- can be explained by denitrification fueled by abundant labile organic matter. Leaky sewage pipes will supply Cl^- and organic carbon, which will alleviate the organic carbon limitation. Whereas denitrification at location MW-D may be enhanced

by the presence of organic matter, the remaining locations likely rely on a limited supply of organic matter in the groundwater.

Where denitrification is fueled by organic matter oxidation, it will likely affect the stable carbon isotopes of DIC. Stable carbon isotope values of groundwater DIC are typically influenced by the type of vegetation and native carbonate minerals (Nascimento et al., 1997). The $\delta^{13}C_{DIC}$ for groundwater at the site averaged -11.9±2.5 ‰, however, the $\delta^{13}C_{DIC}$ shows a pattern of depletion as groundwater travels across the site (Fig. 6). The $\delta^{13}C$ of soil carbonates below the groundwater table averaged -4.1±0.7 ‰, while the values for vegetation can be expected to average about -25‰ because of dominance of C3 type vegetation in temperate regions (Baskaran, 2011). As groundwater enters the site the relatively enriched $\delta^{13}C_{DIC}$ values suggest primary influence from carbonate dissolution with average values at MW-G and MW-H of -8.5±1.1 and -8.3±0.4, respectively. As groundwater exits the study area, the average $\delta^{13}C_{DIC}$ values become more depleted, indicating increased influence from C3 type organic carbon contribution, decreasing average $\delta^{13}C_{DIC}$ values to -13.7±1.6 for MW-C and -12.8±0.7 for MW-D. Upgradient locations MW-G and MW-H and midgradient location MW-A exhibit relatively stable $\delta^{13}C_{DIC}$ compositions over time, whereas MW-B, MW-E, MW-F and MW-C show periodic decreases in $\delta^{13}C_{DIC}$ (Fig. 6) as in nitrate (Fig. 3). These pulses of $\delta^{13}C_{DIC}$ enrichment and depletion may indicate site specific conditions that affect denitrification and carbonate weathering. The $\delta^{13}C_{DIC}$ at MW-C is depleted, suggesting high organic matter degradation. Groundwater at location MW-D is the only location which $\delta^{13}C_{DIC}$ values can be observed to consistently decrease, which suggest cumulative input of a source depleted in $\delta^{13}C$ (Fig. 6). This depleted source of $\delta^{13}C$ is likely related

to the input of organic matter from the leaky sewer that may be degraded to fuel denitrification.

5.3. Effects of nitrification and denitrification on groundwater chemistry

The degree of spatial variations of the measured parameters can be examined using the spatial relative standard deviation (RSD-s) (Fig. 8). A low RSD-s indicates that the parameter in question, and the processes which control it, are relatively uniform throughout the study site. Whereas a higher RSD-s indicates the parameters vary greatly between one sampling location and another. The significance of spatial variations (RSD-s) can be broken into three groups, low variation, medium variation, and high variation (Fig. 8). Variation classifications were defined by observing variations of the parameters relative to the variation of all parameters. Low variability was defined as an RSD-s less than 40%, medium variability was classified as RSD-s less than 90% but greater than 40%, and high variability was defined as RSD-s greater 90%.

The highest spatial variability occurs for NO_3^- and Cl^- concentrations, while pH, pCO_2, and $\delta^{13}C_{DIC}$ are associated with the lowest variability (Fig. 8). The high RSD-s of NO_3^- shows that the NO_3^- contamination in groundwater exhibits steep spatial gradients. High spatial variability in Cl^- can be explained by the influx of Cl^- at location MW-D and at no other location. If location MW-D is not considered, the RSD-s of Cl^- decreases to medium variability; the remaining spatial variability is likely because of dilution occurring at midgradient locations MW-B and MW-E. The low RSD-t and RSD-s of pH indicates that the aquifer is well buffered, whereas the low RSD-s of pCO_2 and $\delta^{13}C_{DIC}$ indicate that the processes which control these parameters are ubiquitous across the site. If denitrification is active, the microbial degradation of organic matter will add lighter

isotopes of carbon to groundwater DIC. If only oxidation of organic matter, with no effects from denitrification, affected $\delta^{13}C_{DIC}$ and pCO_2, we would expect to observe decrease in $\delta^{13}C_{DIC}$ and increase in pCO_2.

If processes which control NO_3^- distribution affects carbonate dissolution, the products and reactants will co-vary (Schot and Pieber, 2012).Thus, if DIC, Ca^{2+}, Mg^{2+} and HCO_3^- are related to denitrification and nitrification, it would be expected that the spatial variability of nitrification and denitrification would increase the RSD of the products of carbonate dissolution. Dissolved inorganic carbon, Ca^{2+}, Mg^{2+} and HCO_3^- exhibit medium variability, confirming that processes which alter their concentrations are not uniform within the groundwater across the sampling locations (Fig. 8).

Similarly, the temporal relative standard deviation (RSD-t) of the measured parameters can be used to determine how the processes which affect those parameters vary over time (Fig. 8). Nitrate and Cl^- also exhibit the highest variation in regards to time. The high RSD-t of NO_3^- is likely because of the periodic pulses from on-site application of fertilizers. High RSD-t of Cl^- indicates that the contamination from sewage occurs periodically. Temporal variability of Cl^- may be explained by short periods where the water table is above the sewer depth, thus reducing the influx of sewage into the groundwater (Table S1). The temporal variability of Cl^- would also be affected by individual rain events causing dilution at locations MW-B and MW-E. The chemical parameters which are directly affected by denitrification (pH and pCO_2) show the least temporal variability (Fig. 8). Low temporal variability of denitrification indicates that the process is relatively constant where it occurs. Products of carbonate dissolution, DIC, Ca^{2+}, Mg^{2+} and HCO_3^- exhibit low to medium temporal variability, which indicates that

the processes controlling these parameters increases and decreases over time. If periodic pulses of NO_3^- contamination affect the activity of denitrification and subsequently carbonate dissolution, it would be expected that the products of carbonate dissolution would show temporal variation.

In order to compare spatial and temporal variability of the groundwater chemistry, RSD-s and RSD-t were compared directly in Fig. 8. RSD-s exhibits approximately twofold higher magnitude than RSD-t, suggesting a greater variability between monitoring wells than variations for each monitoring well over time. The relationship between RSD-s and RSD-t for select geochemical parameters shows a positive correlation with an R^2 of 0.85 using the least squares regression (Fig. 8). The high correlation between the spatial and temporal RSD indicates that as parameters vary spatially across the site, within those specific locations the concentrations are not constant. This leads to the observation that the major ions, HCO_3^- and DIC all exhibit steep spatial gradients because of factors affecting the processes occurring at specific sampling locations.

The major anion in the groundwater was HCO_3^- (Fig. 7) which suggests that the groundwater at the site is dominated by processes controlled by carbonate chemistry. Concentrations of HCO_3^- were highest in the groundwater at downgradient locations MW-C and MW-D. Since HCO_3^- is a byproduct of carbonate weathering and denitrification, it is likely that denitrification has increasing influence on groundwater chemistry as groundwater travels downgradient. If denitrification was occurring but limited, high concentrations of NO_3^- would persist, with concurrent production of CO_2 and HCO_3^-. Such is the case at locations MW-D and MW-C where NO_3^- concentrations at

MW-D are much lower than MW-C, because of the limited availability of organic carbon as an electron donor at MW-C. However, MW-C exhibits higher concentrations of HCO_3^- and depleted $\delta^{13}C_{DIC}$ values compared to upgradient locations, suggesting denitrification does affect the groundwater at this location. The $\delta^{13}C$ from organic carbon degraded and carbonate weathering can be estimated by assuming equal $\delta^{13}C$ contribution from carbonates (-4‰) and the C3 vegetation being consumed during denitrification (-25‰) which would result in a -14.5‰ shift. It can be observed that the downgradient locations, which would most be affected by denitrification the $\delta^{13}C_{DIC}$ shift towards -14.5‰.

Weathering of calcite as the primary form of carbonate dissolution can be confirmed by the use of the saturation index with respect to calcite (SI_{Ca}). Across the study site, the average value for SI_{cal} is -0.9±0.9. Monitoring well-G, MW-H and MW-D show instances where the groundwater is saturated with respect to calcite, but on average, all groundwater is slightly undersaturated with respect to calcite with no spatial or temporal trend. The correlation coefficient (R) between pCO_2 and DIC is 0.65, and the correlation between DIC with HCO_3^- and DIC with Ca^{2+} are 0.93 and 0.81, respectively (Table 2). Weathering of carbonates can be shown through the positive relationship between Ca^{2+} and HCO_3^- in Figure 10c. These relationships indicates that processes which increase $CO_{2(aq)}$, such as nitrification and denitrification, in turn fuel carbonate dissolution in groundwater at this site.

CHAPTER VI

CONCLUSION

In this study, we investigated the spatial and temporal variability of NO_3^- distributions in shallow groundwater at a residential site. The physical, chemical, and isotopic composition of groundwater was used to characterize the processes occurring within the aquifer.

We used observations of the spatial differences between groundwater entering the site, midway at the site, and as it exited the site to attribute NO_3^- contamination to three sources. There was NO_3^- contamination from upgradient application of fertilizers at residences, from application of fertilizers on-site, and from a leaky sewer line. Our results show that denitrification is not occurring uniformly in groundwater across the site, instead, steep NO_3^- gradients exist across the site. Denitrification was found to have varying degrees of activity, most active at the sewage leak and least active in the upgradient groundwater. Factors affecting NO_3^- distributions were runoff from downspouts which resulted in dilution, application of fertilizer at specific locations, and denitrification occurring at different magnitudes. Availability of organic matter appeared to play a key role in the attenuation of NO_3^- by denitrification at some locations.

The processes of nitrification and denitrification had substantial impact on aquifer chemistry through the production of $CO_{2(aq)}$ and subsequent weathering of carbonates.

The relationship between the $CO_{2(g)}$ produced during nitrification and denitrification and the concentrations of HCO_3^- and Ca^{2+} indicates a connection between processes controlling nitrogen and the weathering of carbonates within the aquifer. Groundwater values for the $\delta^{13}C_{DIC}$ indicate DIC is dominated by the dissolution of carbonates and the input of organic matter from C3 type vegetation.

We conclude that denitrification is the dominant method of NO_3^- attenuation occurring at the site and that the $CO_{2(aq)}$ by-product of denitrification enhances carbonate weathering within the aquifer. This work provides valuable insight into the effects residential land use may have on NO_3^- contamination.

CHAPTER VII

FUTURE WORK

This research site has been the subject of previous hydrogeological and geochemical studies (Hagen, 1986; Hoyle, 1989; Pettyjohn, 1989a; Pettyjohn, 1989b). However, it retains potential for use in further elucidating the fate of nitrate in a shallow aquifer. One major shortcoming of this study was the frequency of the sampling. By performing a higher frequency sampling regime, short and long term effects from individual precipitation events on NO_3^- contamination can be investigated. This project can also be converted into a long term study of nitrate contamination and attenuation. This would in turn enhance our understanding and augment our ability to minimize impacts from agricultural and residential contamination in shallow groundwater. Some studies have suggested soil moisture plays an important role in denitrification (Rivett et al., 2008). Continuous measurements of chemical and isotopic parameters during and following a high intensity rain event should provide insights into the process of denitrification as soil moisture changes. In addition to higher frequency and extended sampling, future studies could quantify the rate of nitrification and denitrification through laboratory incubations and in-situ measurements of N_2 and N_2O and stable nitrogen isotopes ($\delta^{15}N$).

REFERENCES

Ali, H.N., Atekwana, E.A., 2011. The effect of sulfuric acid neutralization on carbonate and stable carbon isotope evolution of shallow groundwater. Chemical Geology, 284(3–4): 217-228.

Aravena, R., Robertson, W.D., 1998. Use of Multiple Isotope Tracers to Evaluate Denitrification in Ground Water: Study of Nitrate from a Large-Flux Septic Sytem Plume. Ground Water, 36(6): 975-982.

Asuero, A.G., Sayago, A., González, A.G., 2006. The Correlation Coefficient: An Overview. Critical Reviews in Analytical Chemistry, 36(1): 41-59.

Atekwana, E.A., Krishnamurthy, R.V., 1998. Seasonal variations of dissolve inorganic carbon and $\delta^{13}C$ of surface waters: application of a modified gas evolution technique. Journal of Hydrology, 205: 265-278.

Baskaran, M., 2011. Handbook of Environmental Isotope Geochemistry. Advances in Isotope Geochemistry, Vol I. Springer, New York.

Böhlke, J.-K., 2002. Groundwater recharge and agricultural contamination. Hydrogeology Journal, 10(1): 153-179.

Brunet, F., Potot, C., Probst, A., Probst, J.L., 2011. Stable carbon isotope evidence for nitrogenous fertilizer impact on carbonate weathering in a small agricultural watershed. Rapid Communications in Mass Spectrometry, 25(19): 2682-2690.

Burow, K.R., Nolan, B.T., Rupert, M.G., Dubrovsky, N.M., 2010. Nitrate in Groundwater of the United States, 1991−2003. Environmental Science & Technology, 44(13): 4988-4997.

Canfield, D.E., Glazer, A.N., Falkowshi, P.G., 2010. The Evolution and Future of Earth's Nitrogen Cycle. Science, 330: 192-196.

Davidson, E.A., Stark, J.M., Firestone, M.K., 1990. Microbial Production and Consumption of Nitrate in an Annual Grassland. Ecology, 71(5): 1968-1975.

Delwiche, C.C., Bryan, B.A., 1976. Denitrification. Annual Review of Microbiology, 30: 241-262.

Drever, J.I., 1997. The Geochemistry of Natural Waters: Surface and Groundwater Environments, Upper Saddle River, NJ. Prentice Hall.

Fedstats; 9-2-2013. Map Stats. United States Government, Statistical Programs of The United States Government, http://www.fedstats.gov/qf/states/40/4070300.html, 9-2-13

Goodale, C.L. et al., 2009. Unusual seasonal patterns and inferred processes of nitrogen retention in forested headwaters of the Upper Susquehanna River. Biogeochemistry, 93(3): 197-218.

Green, C.T., Böhlke, J.K., Bekins, B.A., Phillips, S.P., 2010. Mixing effects on apparent reaction rates and isotope fractionation during denitrification in a heterogeneous aquifer. Water Resources Research, 46(8): 19 pp.

Hach, 2013. Digital Titrator Model 16900. Hach Company.

Hagen, D.J., 1986. Spatial and Temporal Variability of Ground-water Quality in a Shallow Aquifer in North-central Oklahoma, Oklahoma State University, 192 pp.

Hounslow, A., 1995. Water quality data: Analysis and interpretation. Lewis Publishers, Boca Raton, FL.

Hoyle, B.L., 1989. Ground-Water Quality Variations in a Silty Alluvial Soil Aquifer, Oklahoma. Ground Water, 27(4): 540-549.

Kite-Powell, A.C., Harding, A.K., 2006. Nitrate Contamination in Oregon Well Water: Geologic Variability and the Public's Perception. Journal of the American Water Resources Association, 42(4): 975-987.

Knowles, R., 1982. Denitrification. Microbilogical Reviews, 46(1): 43-70.

Kuenen, J.G., Robertson, L.A., 1994. Combined nitrification-denitrification processes. FEMS Microbiology Reviews, 15(2-3): 109-117.

Langmuir, D., 1971. The geochemistry of some carbonate ground waters in central Pennsylvania. Geochimica et Cosmochimica Acta, 35(10): 1023-1045.

Lloyd, D., 1993. Aerobic denitrification in soils and sediments: From fallacies to factx. Trends in Ecology & Evolution, 8(10): 352-356.

Lofton, D.D., Hershey, A.E., Whalen, S.C., 2007. Evaluation of Denitrification in an Urban Stream Receiving Wastewater Effluent. Biogeochemistry, 86(1): 77-90.

Lovett, G.M., Likens, G.E., Buso, D.C., Driscoll, C.T., Bailey, S.W., 2005. The Biogeochemistry of Chlorine at Hubbard Brook, New Hampshire, USA. Biogeochemistry, 72(2): 191-232.

Mastrocicco, M., Colombani, N., Castaldelli, G., Jovanovic, N., 2011. Monitoring and Modeling Nitrate Persistence in a Shallow Aquifer. Water, Air and Soil Pollution, 217(1-4): 83-93.

Mesonet; 2014. Daily Precipitation. Oklahoma Mesonet, http://www.mesonet.org/, 9-9-2013

Nascimento, C., Atekwana, E.A., Krishnamurthy, R.V., 1997. Concentrations and isotope ratios of dissolved inorganic carbon in denitrifying environments. Geophysical Research Letters, 24(12): 1511-1514.

Palta, M.M., 2012. Denitrification in Urban Brownfield Wetlands, The State University of New Jersey - Rutgers, 153 pp.

Panno, S.V., Kelly, W.R., Martinsek, A.T., Hackley, K.C., 2006. Estimating Background and Threshold Nitrate Concentrations Using Probability Graphs. Ground Water, 44(5): 697-709.

Parkhurst, D.L., 1995. User's guide to PHREEQC: A computer program for speciation, batch-reaction, one-dimensional transport, and inverse geochemical calculations. U.S. Geological Survey, Water Resource Inversigation Report-4227: 143 pp.

Pettyjohn, W.A., 1989a. Cause and Effect of Rapid Changes in Shallow Groundwater Quality. Oklahoma State University, School of Geology: 21 pp.

Pettyjohn, W.A., 1989b. Field testing some hydrogeologyic assumptions. Journal of applied ground-water protection, 1(2): 4-25.

Rivett, M.O., Buss, S.R., Morgan, P., Smith, J.W.N., Bemment, C.D., 2008. Nitrate attenuation in groundwater: A review of biogeochemical controlling processes. Water Research, 42(16): 4215-4232.

Robertson, G.P., Vitousek, P.M., 2009. Nitrogen in Agriculture: Balancing the Cost of an Essential Resource. Annual Review of Environment and Resources, 34(1): 97-125.

Ross, R.R., 1988. Temporal and Vertical Variability of the Soil and Ground-water Geochemistry of the Ashport Silt Loam, Payne County, Oklahoma, Oklahoma State University, 117 pp.

Schot, P.P., Pieber, S.M., 2012. Spatial and temporal variations in shallow wetland groundwater quality. Journal of Hydrology, 422–423(0): 43-52.

Seitzinger, S., 2008. Nitrogen cycle: Out of reach. Nature, 452(7184): 162-163.

Seitzinger, S. et al., 2006. Denitrification across Landscapes and Waterscapes: A Synthesis. Ecological Applications, 16(6): 2064-2090.

Spalding, R.F., Exner, M.E., 1993. Occurrence of Nitrate in Groundwater - A Review. Journal of Environmental Quality, 22: 392-402.

Stuart, D., Schewe, R.L., McDermott, M., 2014. Reducing nitrogen fertilizer application as a climate change mitigation strategy: Understanding farmer decision-making and potential barriers to change in the US. Land Use Policy, 36(0): 210-218.

Trudell, M.R., Gillham, R.W., Cherry, J.A., 1986. An in-situ study of the occurrence and rate of denitrification in a shallow unconfined sand aquifer. Journal of Hydrology, 83(3–4): 251-268.

US-EPA, 1976. National Interim Primary Drinking Water Regulations, U.S. Environmental Protection Agency., Office of Water Supply.

Ward, B.B., Arp, D.J., Klotz, M.G., 2011. Nitrification. American Society for Microbiology

Table 1. Summary statistics of the chemical, physical and isotopic data.

	Water Level (m)	Temp (°C)	SPC (µS/cm)	DO (mg/l)	pH	HCO_3^- (mg/L)	Ca^{2+} (mg/L)	Mg^{2+} (mg/L)	Na^+ (mg/L)	K^+ (mg/L)	Cl^- (mg/L)	SO_4^- (mg/L)	NO_3^- (mg/L)	DIC (mg C/L)	$\delta^{13}C$ (‰)	pCO_2 (atm)	SI_{Ca}	Ca^{2+}/Mg^{2+}
All Wells																		
Mean	2.9	18.6	830.9	3.3	6.4	376.0	62.0	32.5	58.9	0.6	35.4	33.2	36.8	73.3	-11.9	-2.0	-0.9	2.5
St Dev	0.5	3.2	439.7	1.9	0.6	177.1	27.8	18.2	45.4	0.6	47.9	23.3	37.0	37.9	2.5	0.4	0.9	1.4
Range	2.6	15.0	1938.0	7.8	2.9	745.2	114.7	71.3	161.6	3.6	223.2	105.1	213.9	168.8	8.8	1.9	4.7	5.1
Min	1.2	12.5	74.0	0.5	4.5	48.0	11.9	2.5	1.3	0.1	0.6	2.4	0.1	3.1	-16.3	-3.4	-4.2	1.1
Max	3.8	27.5	2012.0	8.3	7.5	793.2	126.6	73.8	162.9	3.6	223.8	107.5	214.0	171.9	-7.5	-1.5	0.6	6.2
MW-G																		
Mean	2.5	20.6	943.0	3.4	6.5	448.1	81.0	43.4	49.4	1.6	29.4	29.0	57.7	87.0	-8.5	-1.8	-0.6	1.9
St Dev	0.6	3.2	57.9	2.8	0.4	25.2	11.3	4.0	2.7	1.1	10.3	5.6	18.3	14.6	1.1	0.2	0.4	0.1
Range	2.1	10.0	236.0	7.8	1.4	92.4	38.6	13.4	9.5	3.3	39.3	23.6	75.7	52.0	4.7	0.8	1.5	0.4
Min	1.2	15.6	793.0	0.5	5.7	399.6	69.8	39.2	45.5	0.4	13.9	22.6	29.4	52.8	-12.1	-2.4	-1.4	1.7
Max	3.2	25.6	1029.0	8.3	7.1	492.0	108.4	52.6	55.0	3.6	53.2	46.2	105.1	104.8	-7.5	-1.5	0.2	2.1
MW-H																		
Mean	2.6	20.4	965.3	3.1	6.8	454.7	61.7	50.3	61.1	0.6	20.0	61.5	47.6	85.7	-8.3	-2.1	-0.4	1.2
St Dev	0.5	3.3	46.4	1.2	0.4	36.9	7.3	5.2	4.1	0.4	5.1	8.6	11.0	11.3	0.4	0.3	0.5	0.1
Range	1.9	11.8	165.0	5.2	1.7	153.6	22.8	17.2	12.3	1.3	15.3	27.1	39.2	42.8	1.6	1.1	2.0	0.5
Min	1.6	15.7	877.0	1.6	5.8	349.2	52.8	41.8	56.6	0.2	11.5	49.8	21.7	56.8	-9.0	-2.7	-1.6	1.1
Max	3.4	27.5	1042.0	6.8	7.5	502.8	75.6	59.0	68.9	1.5	26.8	76.9	60.9	99.6	-7.5	-1.6	0.4	1.6

MW-F																		
Mean	3.1	18.9	729.6	2.3	6.3	336.1	46.7	20.5	86.5	1.0	23.7	41.3	20.5	69.7	-11.4	-1.9	-2.2	2.4
St Dev	0.5	1.7	304.7	1.2	0.6	121.4	15.1	7.5	47.5	0.2	16.1	22.8	11.3	18.0	1.8	0.2	1.1	0.4
Range	1.6	5.4	938.0	4.5	1.9	382.8	65.7	28.0	147.7	0.6	59.7	66.5	42.9	58.9	5.1	0.8	3.4	1.3
Min	2.2	16.0	223.0	0.5	5.2	99.6	20.0	8.0	5.8	0.6	0.7	3.8	2.6	41.7	-14.4	-2.3	-4.2	1.8
Max	3.8	21.4	1161.0	5.0	7.1	482.4	85.7	36.0	153.5	1.3	60.4	70.3	45.5	100.6	-9.3	-1.5	-0.8	3.2
MW-A																		
Mean	3.0	18.7	878.1	2.9	6.3	404.8	78.0	33.1	42.8	0.2	16.2	21.8	77.9	79.3	-11.5	-1.8	-1.2	2.3
St Dev	0.5	2.4	89.2	1.5	0.3	30.1	12.7	4.6	9.4	0.0	11.6	5.8	38.4	14.6	0.5	0.2	0.8	0.1
Range	1.5	6.6	292.0	4.4	1.2	106.8	47.2	18.0	24.6	0.2	35.7	20.5	151.8	53.7	2.0	0.6	2.7	0.6
Min	2.2	15.2	740.0	1.1	5.6	346.8	50.5	21.7	32.7	0.2	5.1	13.9	36.5	44.9	-12.2	-2.2	-2.8	2.0
Max	3.7	21.8	1032.0	5.4	6.8	453.6	97.7	39.8	57.2	0.3	40.8	34.4	188.3	98.6	-10.2	-1.6	-0.1	2.6
MW-B																		
Mean	2.9	19.8	185.0	4.5	5.9	94.8	26.8	4.8	2.6	0.7	2.0	4.1	7.0	19.4	-14.6	-2.4	-1.5	5.5
St Dev	0.5	3.8	66.5	2.3	0.9	32.9	9.1	1.5	0.6	0.2	1.3	1.2	3.5	6.8	1.1	0.3	0.7	0.4
Range	1.4	11.2	227.0	7.3	2.6	111.6	30.3	4.9	2.0	0.8	4.1	3.8	11.7	24.5	3.3	1.0	2.2	1.7
Min	2.1	13.4	74.0	0.7	4.5	48.0	11.9	2.5	1.9	0.4	0.8	2.4	2.3	10.6	-15.9	-3.0	-2.7	4.5
Max	3.6	24.5	301.0	8.0	7.2	159.6	42.2	7.4	3.9	1.2	5.0	6.2	14.0	35.1	-12.6	-1.9	-0.5	6.2

MW-E																		
Mean	2.8	17.6	216.4	3.5	6.5	133.6	27.3	11.1	2.0	0.2	2.6	6.3	4.8	28.0	-14.5	-2.7	-0.8	2.6
St Dev	0.5	3.3	59.4	1.9	0.7	24.1	4.2	3.2	0.7	0.1	1.6	2.2	3.3	36.2	1.0	0.5	0.3	0.5
Range	1.6	11.3	209.0	5.5	2.1	69.6	13.6	10.7	1.8	0.2	4.8	6.6	9.8	133.9	3.0	1.4	1.2	1.6
Min	1.9	13.5	79.0	1.1	5.3	96.0	20.0	6.4	1.3	0.1	0.6	3.2	0.2	3.1	-16.3	-3.4	-1.4	1.9
Max	3.5	24.9	288.0	6.6	7.4	165.6	33.6	17.1	3.1	0.3	5.4	9.8	10.0	137.0	-13.2	-2.0	-0.3	3.5
MW-D																		
Mean	3.0	16.6	1523.4	3.5	6.7	605.4	104.4	46.9	134.0	0.3	145.4	60.1	4.7	120.4	-12.8	-1.9	-0.2	2.4
St Dev	0.5	2.4	183.1	1.9	0.3	61.9	15.0	11.2	16.9	0.1	48.7	17.7	2.8	20.1	0.7	0.2	0.4	1.1
Range	1.8	6.9	801.0	6.7	1.3	223.2	52.3	36.2	48.5	0.3	150.8	80.3	8.8	68.1	2.2	0.9	1.4	3.9
Min	1.9	12.9	1211.0	0.9	6.2	450.0	74.3	24.3	114.4	0.1	73.0	27.2	0.1	78.8	-14.1	-2.4	-0.8	1.3
Max	3.7	19.7	2012.0	7.6	7.4	673.2	126.6	60.5	162.9	0.5	223.8	107.5	8.9	146.9	-11.9	-1.5	0.6	5.2
MW-C																		
Mean	2.9	16.1	1095.6	3.2	6.5	490.2	64.4	47.5	79.6	0.4	38.2	38.1	66.8	100.8	-13.7	-1.9	-0.7	1.4
St Dev	0.5	2.1	210.4	1.7	0.4	121.8	17.8	13.3	20.1	0.1	17.1	11.8	48.9	34.9	1.6	0.2	0.4	0.1
Range	1.6	6.9	756.0	6.0	1.5	436.8	70.4	47.7	83.8	0.4	66.9	42.9	194.6	112.7	5.0	0.7	1.6	0.6
Min	2.0	12.5	825.0	1.2	5.6	356.4	33.6	26.1	41.2	0.2	14.3	19.9	19.4	59.2	-16.1	-2.2	-1.7	1.1
Max	3.6	19.4	1581.0	7.1	7.0	793.2	104.0	73.8	125.0	0.7	81.3	62.8	214.0	171.9	-11.1	-1.5	-0.1	1.7

DO = dissolved oxygen, Temp = temperature, ORP = oxidation reduction potential, DIC = dissolved inorganic carbon, pCO_2 = partial pressure of CO_2 calculated using DIC, Si_{Ca} = the saturation index with respect to calcite, $\delta^{13}C$ from DIC, St Dev is standard deviation.

Table 2 correlation coefficient of the chemical physical and isotopic data.

	Water Level (m)	*Temp (°C)*	*SPC (µS/cm)*	*DO (mg/L)*	*pH*	*ORP (mV)*	Ca^{2+} (mg/L)	Mg^{2+} (mg/L)	Na^{+} (mg/L)	K^{+} (mg/L)	HCO_3^{-} (mg/L)	Cl^{-} (mg/L)	SO_4^{-} (mg/L)	NO_3^{-} (mg/L)	DIC (mg C/L)	$\delta^{13}C_{DIC}$ (‰)	Log pCO_2	SI_{Ca}	Ca^{2+}/Mg^{2+}
Water Level	1.00																		
Temp	0.36	1.00																	
SPC	-0.03	-0.21	1.00																
DO	0.07	0.06	-0.17	1.00															
pH	0.05	-0.07	0.37	-0.24	1.00														
ORP	0.01	-0.03	0.17	0.15	-0.10	1.00													
Ca^{2+}	-0.03	-0.12	0.88	-0.08	0.34	0.22	1.00												
Mg^{2+}	-0.18	-0.11	0.86	-0.10	0.37	0.03	0.76	1.00											
Na^{+}	0.05	-0.25	0.88	-0.18	0.30	0.09	0.69	0.66	1.00										
K^{+}	0.02	0.35	-0.08	-0.02	-0.09	-0.22	-0.04	-0.03	-0.02	1.00									
HCO_3^{-}	-0.09	-0.22	0.95	-0.17	0.42	0.05	0.85	0.87	0.83	-0.03	1.00								
Cl^{-}	0.02	-0.27	0.78	-0.05	0.24	0.27	0.71	0.49	0.76	-0.18	0.63	1.00							
SO_4^{-}	-0.11	-0.17	0.80	-0.18	0.37	0.03	0.60	0.74	0.84	0.00	0.79	0.60	1.00						
NO_3^{-}	0.00	0.06	0.26	-0.06	0.06	0.05	0.32	0.41	0.01	0.03	0.25	-0.14	0.05	1.00					
DIC	-0.12	-0.25	0.90	-0.14	0.33	0.11	0.81	0.81	0.77	-0.04	0.93	0.62	0.71	0.23	1.00				
$\delta^{13}C_{DIC}$	-0.20	0.24	0.35	-0.23	0.25	-0.10	0.33	0.46	0.22	0.40	0.42	-0.03	0.43	0.37	0.37	1.00			
Log pCO_2	-0.02	0.03	0.56	-0.07	-0.35	0.11	0.51	0.52	0.48	0.14	0.55	0.29	0.38	0.32	0.65	0.33	1.00		
SI_{Ca}	0.04	-0.05	0.70	-0.27	0.89	-0.03	0.68	0.67	0.57	-0.03	0.75	0.43	0.60	0.24	0.65	0.43	0.06	1.00	
Ca^{2+}/Mg^{2+}	0.14	0.09	-0.58	0.21	-0.32	0.09	-0.39	-0.76	-0.48	0.02	-0.64	-0.16	-0.58	-0.41	-0.57	-0.51	-0.41	-0.53	1.00

DO = dissolved oxygen, ORP = oxidation reduction potential, DIC = dissolved inorganic carbon, $\delta^{13}C$ from dissolved inorganic carbon, pCO_2 = partial pressure of CO_2, SI_{Ca} = the saturation index with respect to calcite. Underlined areas indicate moderately strong correlation.

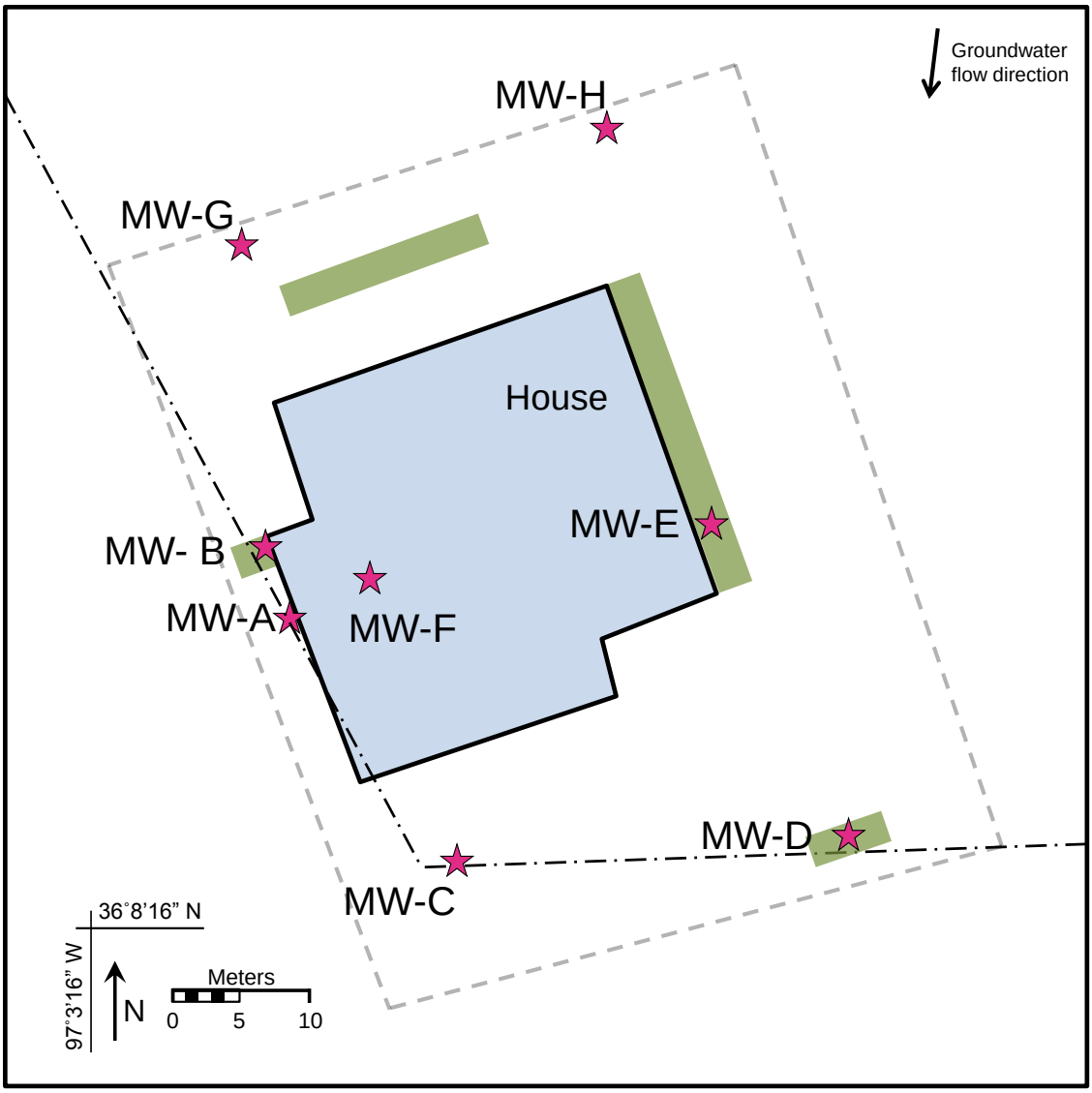

Fig. 1. Study site located in north central Oklahoma, USA. Stars denote monitoring wells (MW). Dashed lines indicate property boundary. Groundwater flow is indicated by the arrow. Shaded rectangles indicate flower beds and the dash-dot line indicates a sewer line.

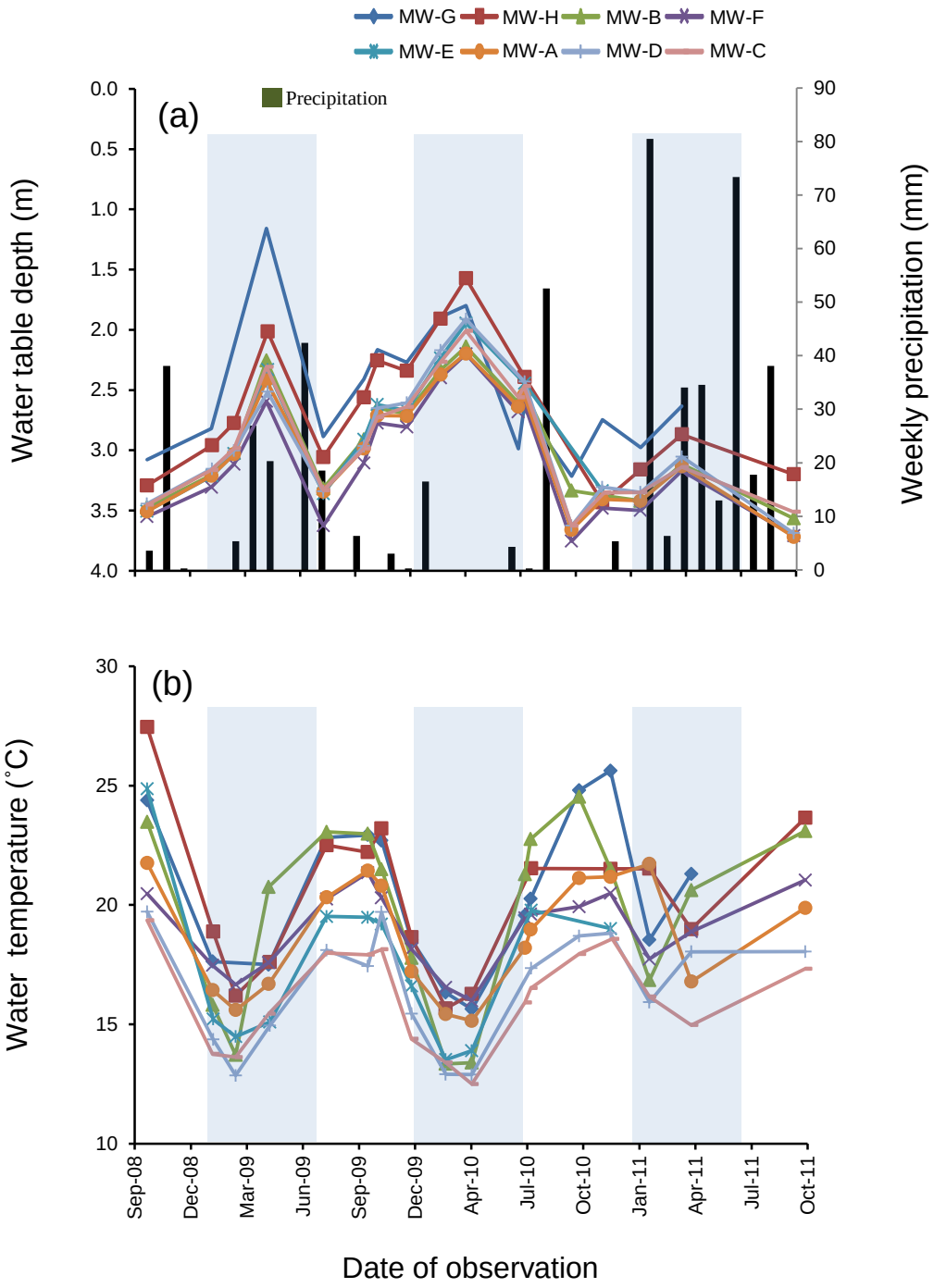

Fig. 2. Plot of the temporal variations in (a) water table depths and mean weekly precipitation and (b) water temperature. Precipitation data is from www.mesonet.org (accessed 12-15-2013). Blue shaded regions indicate high water periods.

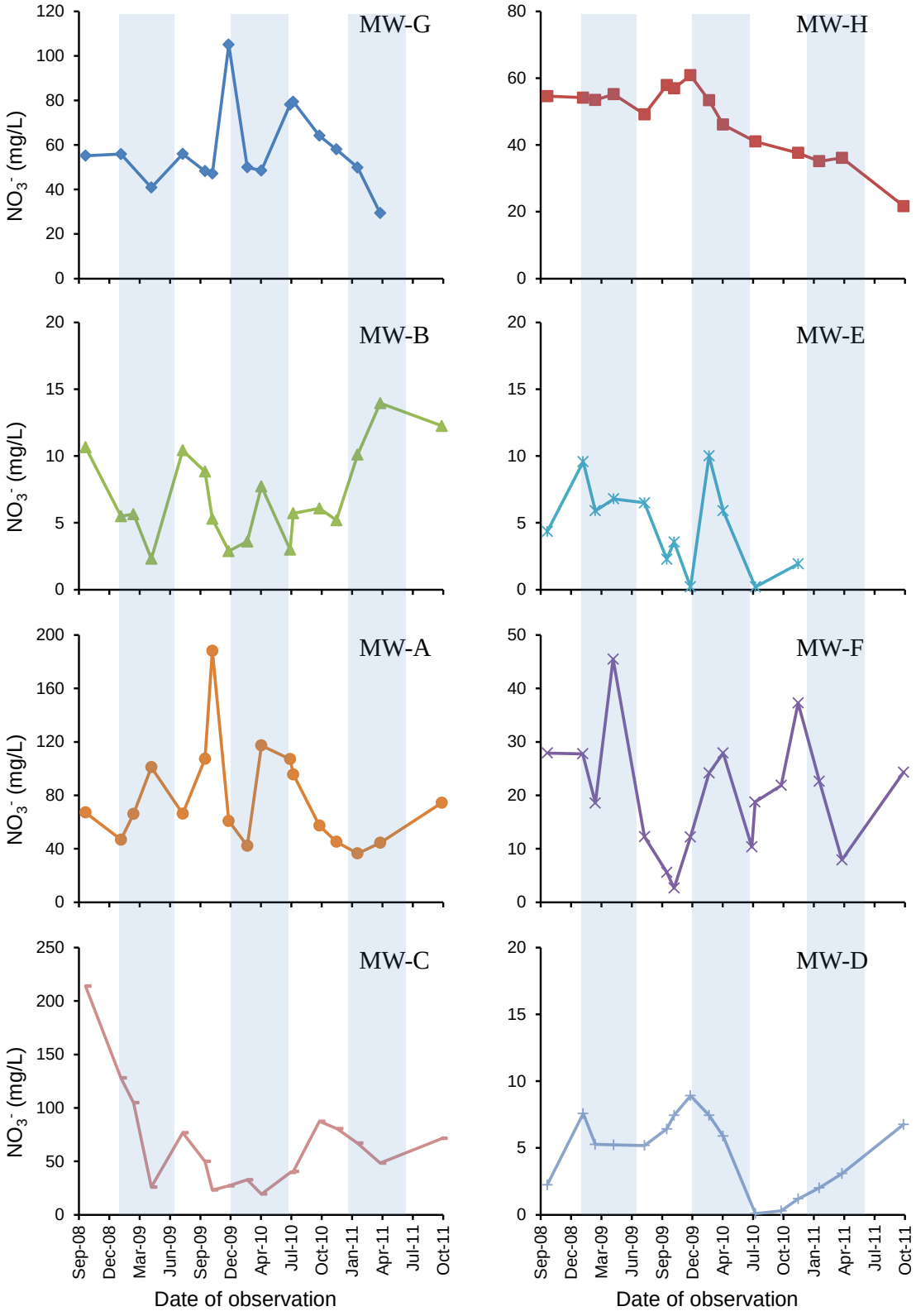

Fig. 3. Plot of the temporal variations in the nitrate concentrations in groundwater. Shaded regions indicate high water periods defined in Fig 2a.

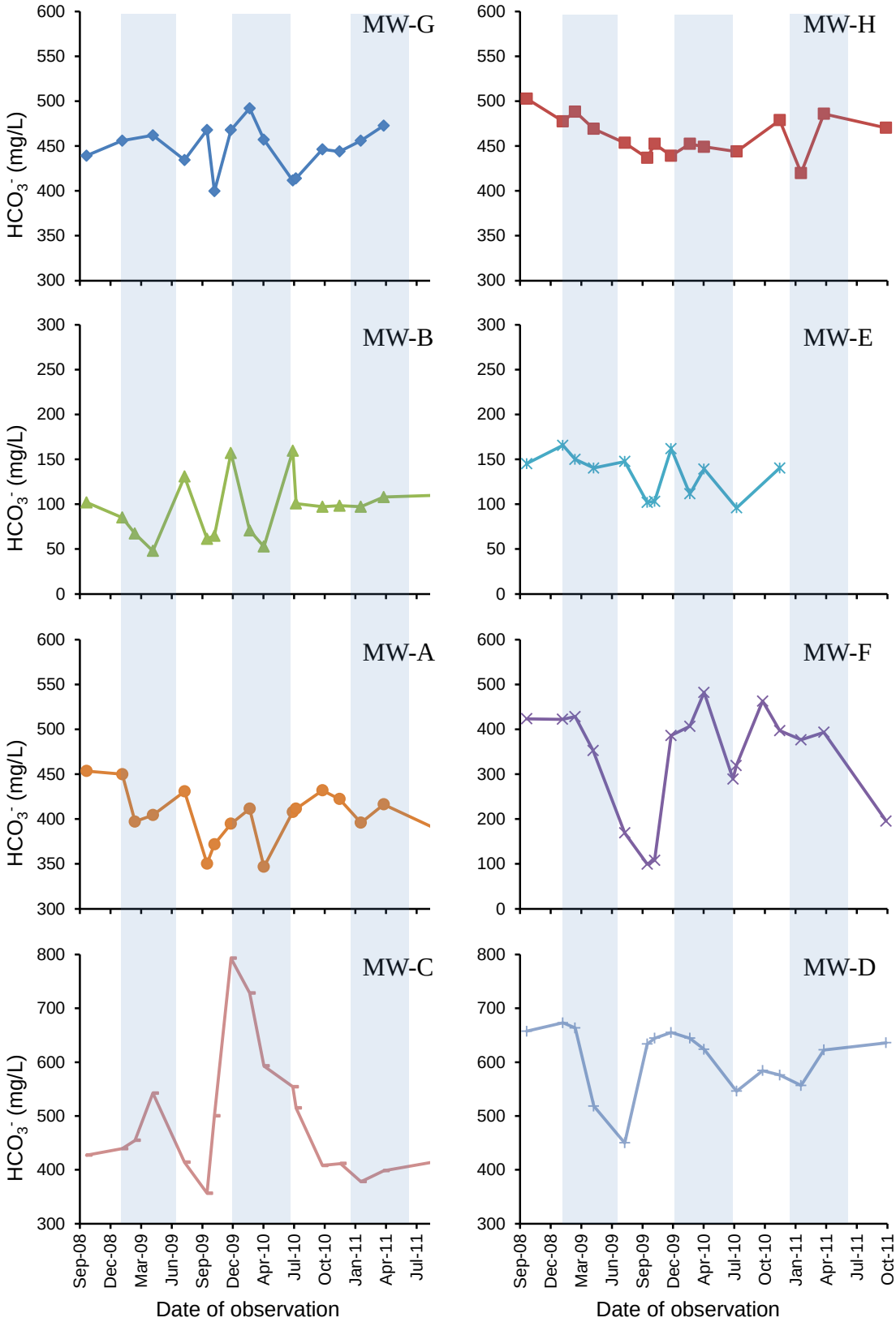

Fig. 4. Plot of the temporal variations in the HCO_3^- (mg/L) concentrations in groundwater. Shaded regions indicate high water periods defined in Fig 2a.

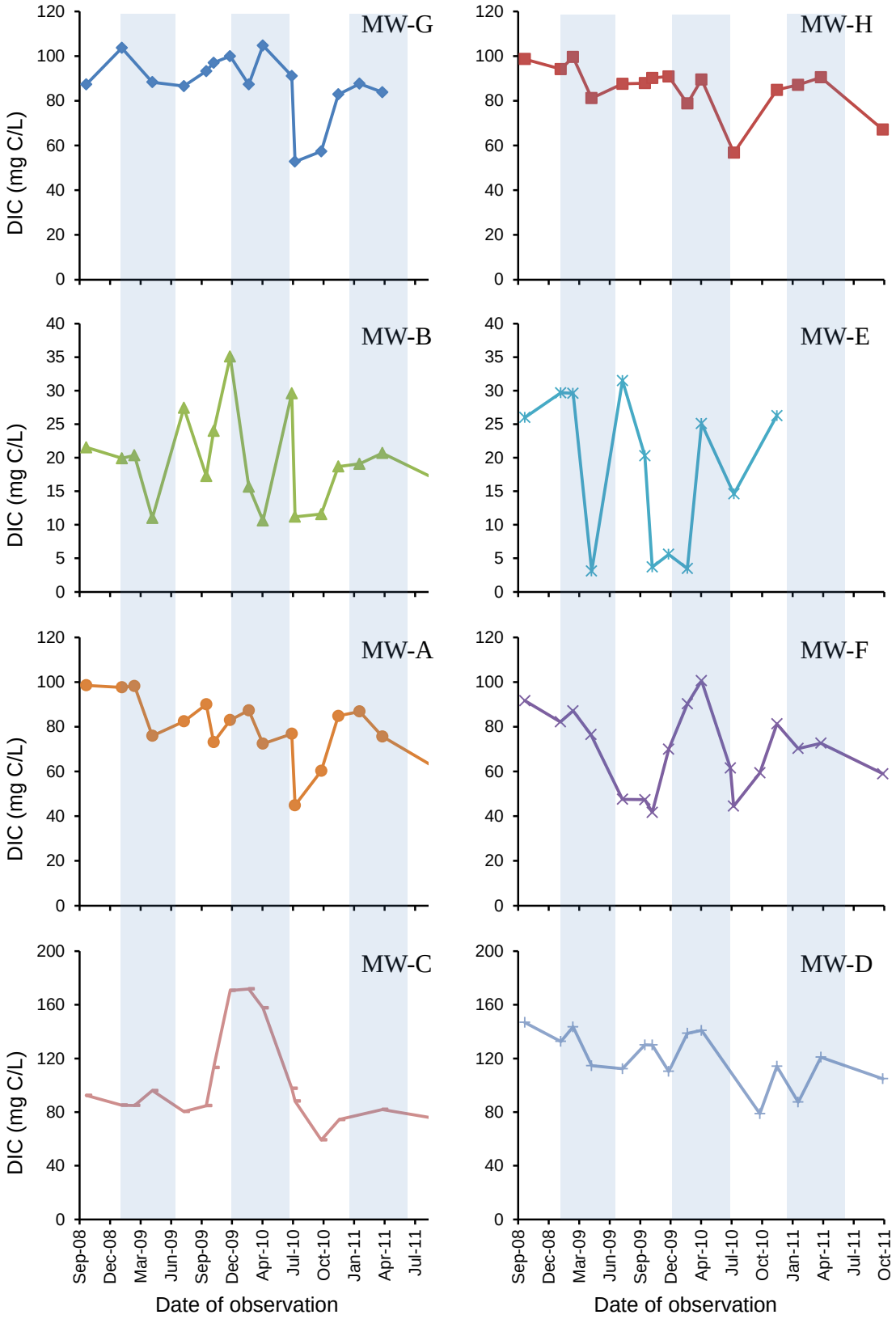

Fig. 5. Plot of the temporal variations in the dissolved inorganic carbon (DIC) concentrations in groundwater. Shaded regions indicate high water periods defined in Fig 2a.

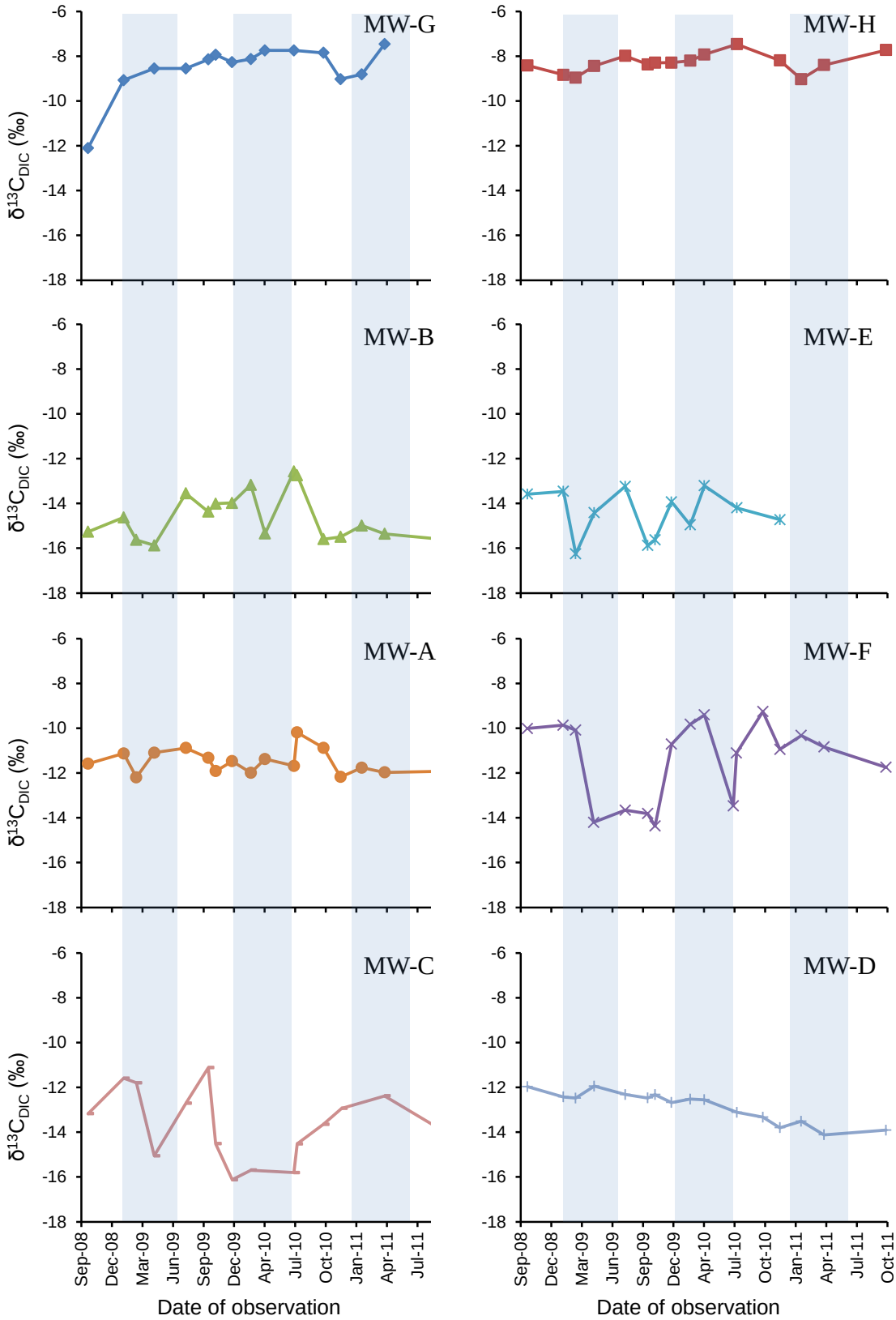

Fig. 6. Plot of the temporal variations in the stable isotopes of dissolved inorganic carbon ($\delta^{13}C_{DIC}$) of groundwater. Shaded regions indicate high water periods defined in Fig 2a.

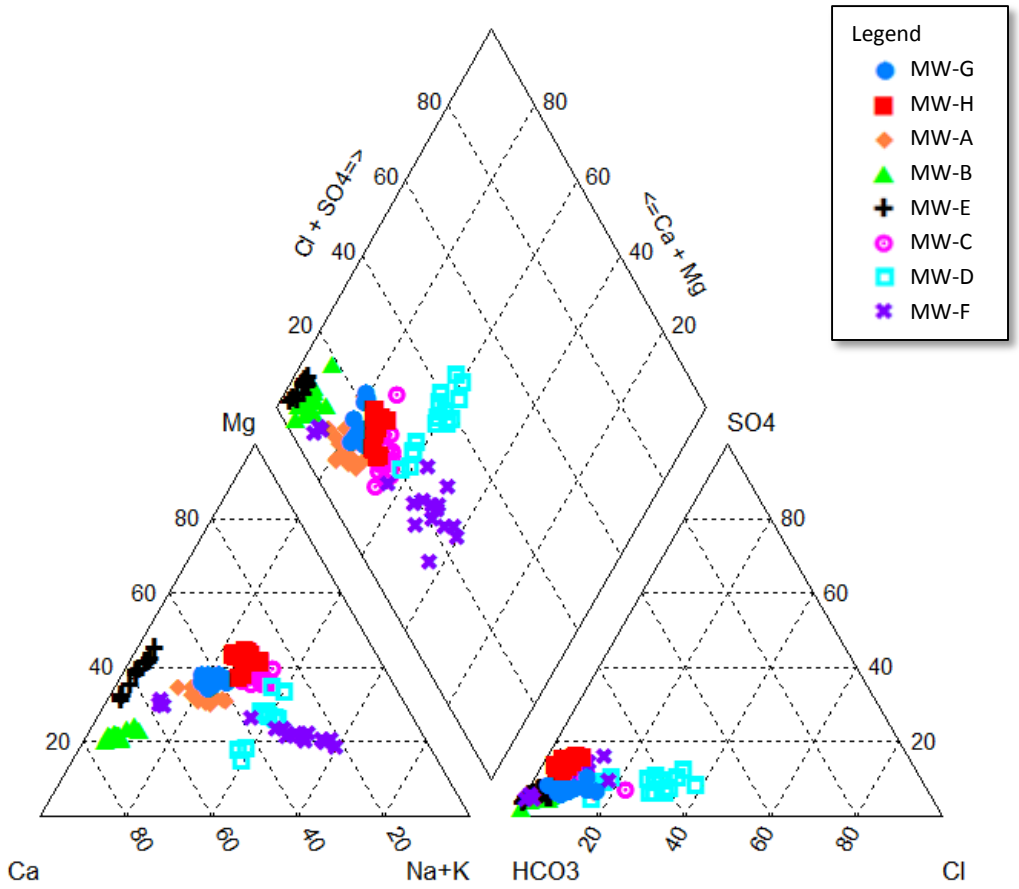

Fig. 7. Piper diagram for major ions in groundwater.

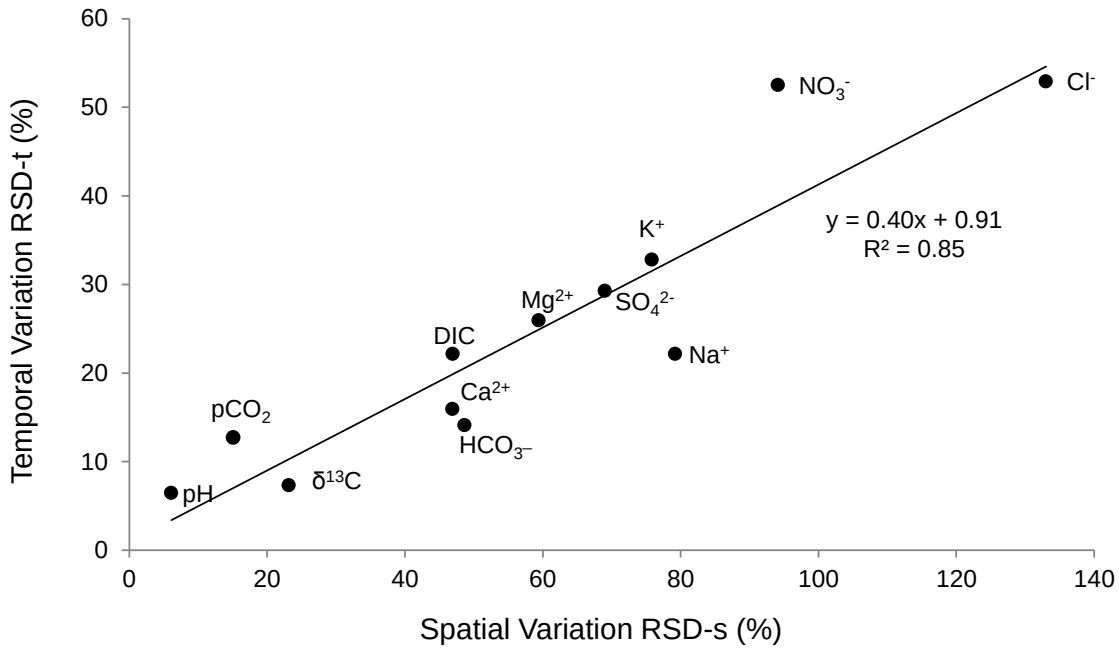

Fig. 8. Linear regression between the spatial relative standard deviation (RSD-s) and temporal relative standard deviation (RSD-t) variations in pH, partial pressure of $CO_{2(g)}$ (pCO_2), stable carbon isotopes of dissolved inorganic carbon (DIC) ($\delta^{13}C_{DIC}$), Ca^{2+}, HCO_3^-, DIC, Mg^{2+}, SO_4^{2-}, K^+, Na^+, Cl^- and NO_3^-.

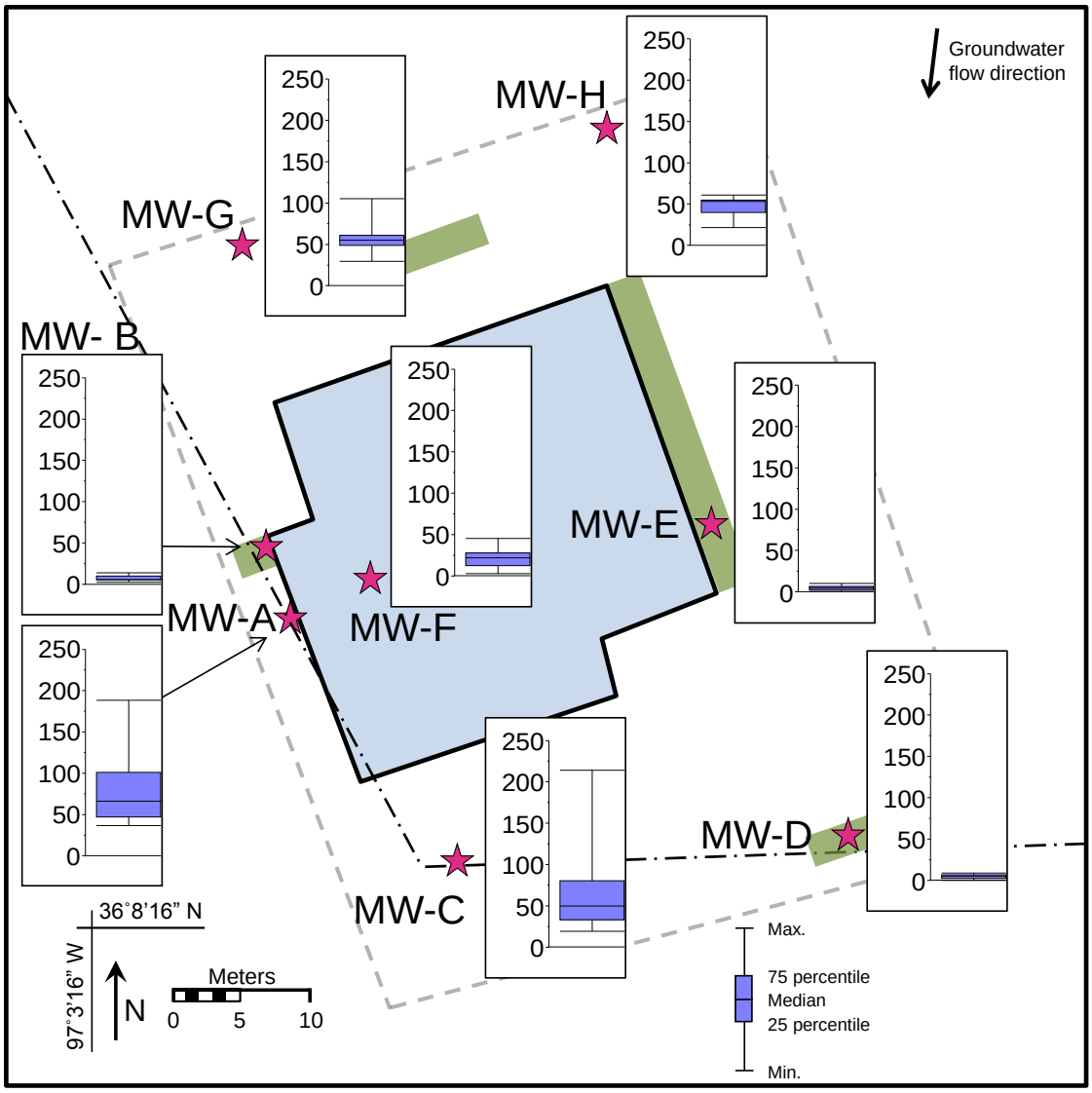

Fig. 9. Box and whisker plots showing the maximum, 75 percentile, medial, 25 percentile, and minimum in the NO_3^- (mg/L) at the study site. The stars denote groundwater sampling locations. Dashed lines indicate property boundary. Shaded rectangles indicate flower beds. The short dash-dot line indicate sewer lines. Groundwater flow is indicated by the arrow.

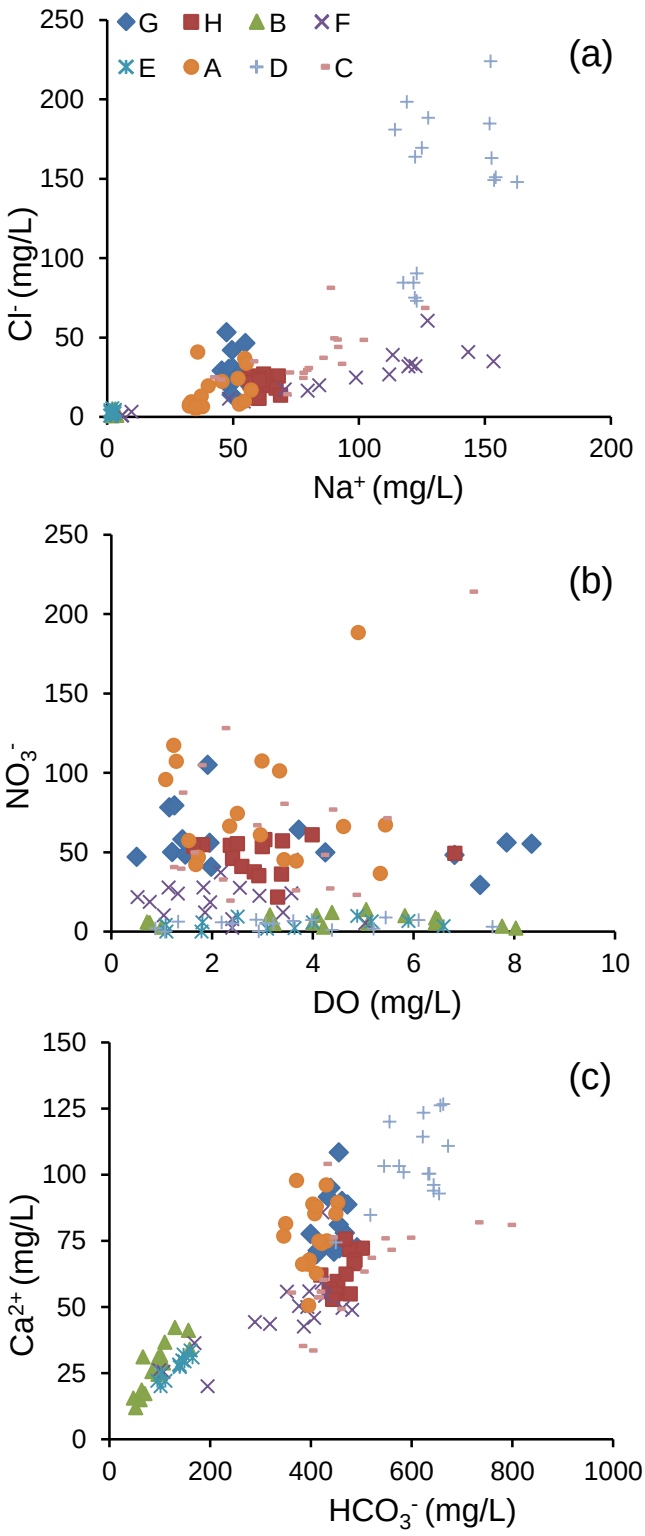

Fig. 10. (a) Comparison of Cl^- to Na^+ concentrations (mg/L). (b) Comparison of NO_3^- to dissolved oxygen (DO) (mg/L). (c) Comparison of Ca^{2+} to HCO_3^- concentrations (mg/L).

APPENDICES

Table S1 Compilation of the chemical physical and isotopic data.

Date	*Water Level*	*Temp*	*SPC*	*DO*	*pH*	*ORP*	Ca^{2+}	Mg^{2+}	Na^{+}	K^{+}	HCO_3^{-}	Cl^{-}	SO_4^{-}	NO_3^{-}	DIC	$\delta^{13}C_{DIC}$	Log pCO_2	SI_{Ca}	Ca^{2+}/Mg^{2+}
	(m)	*(°C)*	*(µS/cm)*	*(mg/L)*		*(mV)*	(mg/L)	(mg/L)	(mg/L)	(mg/L)	(mg/L)	(mg/L)	(mg/L)	(mg/L)	(mg C/L)	(‰)			
MW-G																			
9/30/2008	3.1	24.4	1029	8.3	7.1	69.6	94.9	49.6	47.4	0.4	439.2	53.2	26.8	55.2	87.4	-12.1	-2.2	0.2	1.91
1/19/2009	2.8	17.6	1017	2.0	6.5	77.0	108.4	52.6	55.0	0.6	456.0	46.4	30.5	55.9	103.7	-9.1	-1.8	-0.4	2.06
2/27/2009	ns	ns	ns	ns	ns	ns	ns	ns	ns	ns	ns	ns	ns	ns	ns	ns	ns	ns	ns
4/24/2009	1.2	17.5	1014	2.0	6.3	41.2	90.0	48.6	49.7	0.4	462.0	41.9	46.2	40.9	88.3	-8.5	-1.7	-0.8	1.85
7/31/2009	2.9	22.8	971	7.9	6.1	23.0	91.6	44.5	45.5	1.5	434.4	29.0	25.7	56.0	86.6	-8.5	-1.6	-0.8	2.06
10/9/2009	2.4	22.9	944	6.8	6.8	-14.8	77.9	44.7	49.7	1.4	468.0	26.0	23.6	48.2	93.3	-8.1	-1.9	-0.2	1.74
11/1/2009	2.2	22.7	975	0.5	6.7	29.2	77.5	44.0	49.8	1.0	399.6	23.8	22.6	47.1	97.1	-7.9	-1.9	-0.4	1.76
12/22/2009	2.3	18.5	943	1.9	6.8	111.1	74.7	41.9	48.0	1.7	468.0	27.1	30.9	105.1	100.0	-8.3	-2.0	-0.3	1.78
2/18/2010	1.9	16.3	908	1.2	6.6	-70.9	72.5	41.4	46.8	0.6	492.0	25.5	25.3	49.9	87.4	-8.1	-1.9	-0.5	1.75
4/3/2010	1.8	15.6	905	1.5	6.3	-4.8	72.2	41.2	46.8	0.8	457.2	23.5	25.9	48.5	104.8	-7.7	-1.7	-0.9	1.75
7/2/2010	3.0	19.6	914	1.2	6.6	-106.5	69.8	39.2	48.3	3.6	411.6	30.1	27.7	78.2	91.1	-7.7	-1.8	-0.6	1.78
7/12/2010	2.7	20.3	950	1.3	7.0	4.7	71.3	40.6	49.8	0.9	414.0	31.0	28.4	79.4	52.8	ns	-2.4	-0.1	1.76
10/2/2010	3.2	24.8	942	3.7	6.6	31.6	70.9	40.0	52.0	3.0	446.4	26.0	28.1	64.2	57.4	-7.8	-2.0	-0.4	1.77
11/24/2010	2.7	25.6	928	1.4	6.4	-15.4	73.4	40.6	54.2	2.7	444.0	23.7	28.5	58.0	82.9	-9.0	-1.7	-0.6	1.81
1/29/2011	3.0	18.5	912	4.3	5.7	21.2	81.1	40.1	48.5	1.8	456.0	19.5	31.2	49.9	87.7	-8.8	-1.5	-1.4	2.02
4/10/2011	2.6	21.3	793	7.3	5.7	14.8	88.6	41.4	49.4	3.3	472.8	13.9	33.3	29.4	83.9	-7.5	-1.5	-1.3	2.14
10/20/2011	ns	ns	ns	ns	ns	ns	ns	ns	ns	ns	ns	ns	ns	ns	ns	ns	ns	ns	ns
MW-H																			
9/30/2008	3.3	27.5	1042	1.8	7.1	26.9	72.2	56.5	62.2	0.3	502.8	26.8	70.6	54.6	98.7	-8.4	-2.1	0.1	1.28
1/20/2009	3.0	18.9	1013	2.4	7.4	-33.0	71.6	58.0	68.1	0.3	477.6	25.6	76.9	54.2	94.2	-8.8	-2.4	0.2	1.24
2/27/2009	2.8	16.2	1009	1.6	7.1	73.1	67.6	54.3	56.6	0.2	488.4	25.7	76.7	53.5	99.6	-9.0	-2.2	-0.1	1.25
4/26/2009	2.0	17.6	1006	2.5	6.8	126.7	75.6	59.0	60.6	0.8	469.2	24.3	72.5	55.2	81.2	-8.4	-2.0	-0.3	1.28
7/31/2009	3.1	22.5	1008	6.8	6.2	49.0	57.9	51.1	57.1	0.2	453.6	21.8	57.2	49.2	87.6	-8.0	-1.6	-1.0	1.13
10/9/2009	2.6	22.2	977	3.1	6.8	41.8	55.8	47.6	56.8	0.3	436.8	21.4	54.7	57.9	87.9	-8.4	-1.9	-0.4	1.17
11/1/2009	2.3	23.2	975	3.4	6.6	54.6	59.5	52.5	63.2	0.3	452.4	19.7	53.0	57.0	90.3	-8.3	-1.8	-0.5	1.13
12/22/2009	2.3	18.7	946	4.0	7.1	96.8	56.8	49.9	58.6	0.4	439.2	21.3	61.5	60.9	90.9	-8.3	-2.2	-0.2	1.14
2/18/2010	1.9	15.7	877	3.0	6.6	-90.4	55.2	49.4	57.1	0.8	452.4	21.6	57.4	53.4	78.8	-8.2	-2.0	-0.7	1.12
4/3/2010	1.6	16.3	921	2.4	5.8	6.3	55.0	48.8	60.5	0.4	349.2	23.1	55.3	46.1	89.5	-7.9	-1.6	-1.6	1.13
7/2/2010	ns	ns	ns	ns	ns	ns	ns	ns	ns	ns	ns	ns	ns	ns	ns	ns	ns	ns	ns
7/13/2010	2.4	21.5	953	2.6	7.1	-4.7	52.8	46.9	67.1	0.8	444.0	18.0	49.8	41.0	56.8	-7.5	-2.4	-0.1	1.13
10/2/2010	ns	ns	ns	ns	ns	ns	ns	ns	ns	ns	ns	ns	ns	ns	ns	ns	ns	ns	ns
11/24/2010	3.4	21.5	918	2.8	6.9	-4.8	54.8	49.3	68.9	0.7	478.8	13.6	55.7	37.6	84.9	-8.2	-2.1	-0.3	1.11
1/29/2011	3.2	21.5	985	2.9	7.0	66.8	62.0	47.1	59.1	1.5	420.0	13.8	61.0	35.1	87.2	-9.0	-2.1	-0.2	1.31
4/10/2011	2.9	19.0	934	3.4	6.5	24.1	66.4	41.8	60.2	1.1	486.0	11.9	60.8	36.1	90.5	-8.4	-1.8	-0.6	1.59
10/20/2011	2.3	23.7	916	3.3	7.5	-102.8	62.4	41.8	60.2	1.1	470.4	11.5	59.2	21.7	67.1	-7.7	-2.7	0.4	1.49
MW-B																			
9/30/2008	3.5	23.5	198	3.2	6.3	17.0	31.7	5.5	3.9	0.8	102.0	1.0	3.9	10.7	21.6	-15.3	-2.3	-1.6	5.74
1/19/2009	3.2	15.8	159	6.4	7.2	6.8	25.5	4.6	2.2	0.8	85.2	1.6	5.0	5.5	19.9	-14.6	-3.0	-1.0	5.53
2/27/2009	3.0	13.7	174	4.0	6.1	79.7	31.1	5.3	3.4	0.8	67.2	5.0	5.4	5.6	20.4	-15.6	-2.3	-2.1	5.83
4/24/2009	2.3	20.8	102	8.0	5.3	115.2	15.5	2.8	1.9	0.5	48.0	1.1	2.6	2.3	11.0	-15.9	-2.4	-3.2	5.59
7/31/2009	3.3	23.1	263	4.1	5.0	68.0	42.2	7.3	3.3	0.8	130.8	1.7	4.2	10.4	27.4	-13.6	-1.9	-2.7	5.76
10/9/2009	2.9	23.0	116	6.4	5.0	38.8	14.9	3.3	2.2	0.6	61.4	0.9	3.0	8.8	17.3	-14.4	-2.1	-3.4	4.53
11/1/2009	2.7	21.5	136	5.1	5.2	147.5	18.6	3.8	2.3	0.6	64.8	0.8	2.6	5.3	24.0	-14.0	-2.0	-3.1	4.86
12/22/2009	2.7	17.8	301	4.2	6.9	9.0	41.2	7.4	3.0	0.7	157.2	1.5	4.9	2.9	35.1	-14.0	-2.5	-0.8	5.60

2/18/2010	2.3	13.4	91	7.8	5.7	30.9	17.3	3.1	2.0	0.4	70.8	0.8	2.9	3.6	15.7	-13.2	-2.3	-2.8	5.48
4/3/2010	2.1	13.4	74	6.5	4.5	-16.9	11.9	2.5	2.1	0.6	52.8	1.8	3.1	7.7	10.6	-15.3	-2.4	-4.2	4.75
7/2/2010	2.6	21.3	288	1.0	6.9	-27.1	34.0	6.3	2.9	1.0	159.6	1.0	2.4	3.0	29.6	-12.6	-2.5	-0.8	5.41
7/12/2010	2.5	22.8	188	0.8	6.7	-0.7	25.5	4.6	2.5	0.7	100.8	4.3	3.6	5.7	11.2	-12.7	-2.8	-1.3	5.53
10/2/2010	3.3	24.5	205	0.7	5.6	77.1	24.4	4.4	2.3	1.0	97.2	1.4	4.2	6.1	11.6	-15.6	-2.3	-2.4	5.53
11/24/2010	3.4	21.5	187	3.2	4.8	25.3	25.3	4.7	2.2	0.7	98.4	4.1	4.3	5.2	18.7	-15.5	-2.1	-3.3	5.38
1/29/2011	3.4	16.9	214	5.8	5.4	10.1	30.8	5.0	2.1	0.6	97.2	2.1	5.5	10.1	19.1	-15.0	-2.2	-2.6	6.22
4/10/2011	3.1	20.6	233	5.1	6.5	23.4	28.8	5.0	2.3	0.5	108.0	2.7	5.3	14.0	20.7	-15.4	-2.4	-1.5	5.78
10/20/2011	3.6	23.1	216	4.4	6.9	-107.2	36.6	6.3	2.9	1.2	110.4	3.1	6.2	12.3	16.2	-15.6	-2.8	-0.9	5.83
MW-F																			
9/30/2008	3.6	20.5	1161	1.8	6.7	-53.4	85.7	36.0	127.3	1.0	423.6	60.4	41.0	27.9	91.7	-10.0	-1.9	-0.4	2.38
1/19/2009	3.3	17.5	950	2.6	7.1	60.7	59.1	25.7	120.6	1.1	422.4	33.3	61.5	27.8	82.2	-9.9	-2.3	-0.1	2.30
2/27/2009	3.1	16.7	859	2.0	7.0	75.6	54.2	22.7	112.0	1.1	428.4	26.6	54.7	18.6	87.2	-10.1	-2.2	-0.3	2.39
4/24/2009	2.6	17.6	755	3.6	5.5	84.0	55.7	24.5	113.5	1.1	352.8	39.0	61.3	45.5	76.5	-14.2	-1.6	-1.8	2.27
7/31/2009	3.6	20.3	384	1.9	5.6	37.7	36.3	11.4	9.7	1.1	169.2	3.1	6.2	12.3	47.6	-13.7	-1.8	-2.1	3.19
10/9/2009	3.1	21.4	223	5.0	5.2	225.3	26.0	8.7	6.1	1.0	99.6	0.9	4.7	5.6	47.4	-13.8	-1.7	-2.8	3.00
11/1/2009	2.8	20.3	262	2.4	6.2	116.6	25.4	8.0	5.8	1.2	108.0	0.7	3.8	2.6	41.7	-14.4	-2.0	-1.8	3.17
12/22/2009	2.8	18.2	657	3.4	6.9	120.5	42.6	19.2	79.7	0.9	386.4	16.5	37.6	12.2	70.0	-10.7	-2.2	-0.4	2.22
2/18/2010	2.4	16.6	906	1.3	6.4	-86.5	45.8	23.1	119.7	1.2	406.8	31.7	53.3	24.2	90.3	-9.8	-1.8	-1.0	1.98
4/3/2010	2.2	16.0	1049	1.1	6.2	-26.7	48.9	26.5	143.5	1.3	482.4	40.8	70.3	27.9	100.6	-9.4	-1.6	-1.1	1.85
7/2/2010	2.7	19.5	416	1.0	6.6	3.2	44.3	18.6	48.5	1.0	289.2	11.4	25.6	10.4	61.6	-13.5	-2.0	-0.9	2.38
7/12/2010	2.6	19.6	630	0.8	6.4	8.8	43.5	19.2	70.6	1.1	319.2	17.2	35.5	18.8	44.5	-11.1	-2.0	-1.0	2.27
10/2/2010	3.8	19.9	1137	0.5	6.9	59.6	49.6	25.1	153.5	1.3	463.2	34.9	68.7	21.9	59.4	-9.3	-2.3	-0.3	1.98
11/24/2010	3.5	20.5	983	2.2	5.2	15.5	55.9	27.6	122.5	1.0	397.2	31.8	51.1	37.3	81.3	-10.9	-1.5	-2.0	2.03
1/29/2011	3.5	17.7	857	2.9	6.0	10.0	50.3	22.1	98.9	0.9	376.8	24.7	55.2	22.6	70.3	-10.3	-1.7	-1.3	2.28
4/10/2011	3.2	18.9	816	2.4	6.4	22.9	50.0	19.9	84.3	0.6	393.6	19.9	58.3	7.9	72.7	-10.8	-1.8	-0.9	2.51
10/20/2011	3.7	21.0	358	3.6	6.3	-118.6	20.0	9.9	54.3	0.6	195.6	9.5	13.6	24.3	59.0	-11.7	-1.9	-1.6	2.01
MW-E																			
9/30/2008	3.5	24.9	220	1.1	6.9	-6.0	29.8	13.8	3.0	0.3	145.2	2.1	7.0	4.4	26.0	-13.6	-2.5	-0.9	2.15
1/20/2009	3.2	15.2	260	2.5	7.3	3.9	30.8	14.8	3.1	0.2	165.6	3.5	9.8	9.6	29.7	-13.5	-2.9	-0.5	2.09
2/27/2009	3.0	14.5	262	1.8	7.4	29.8	29.4	12.2	2.1	0.1	150.0	2.7	8.8	5.9	29.6	-16.3	-3.0	-0.5	2.42
4/26/2009	2.3	15.1	196	5.9	6.6	141.7	27.7	10.8	1.9	0.1	140.4	1.1	6.6	6.8	3.1	-14.4	-3.3	-1.4	2.56
7/31/2009	3.4	19.5	288	5.2	5.9	13.8	31.9	17.1	3.1	0.2	147.6	4.3	7.5	6.5	31.5	-13.2	-2.0	-2.0	1.87
10/9/2009	2.9	19.5	176	3.6	5.9	3.2	20.0	9.0	1.7	0.1	102.0	0.6	3.9	2.3	20.3	-15.9	-2.2	-2.3	2.22
11/1/2009	2.6	19.2	179	6.6	6.8	62.3	25.0	7.6	1.3	0.1	103.2	0.8	3.2	3.6	3.7	-15.6	-3.4	-1.2	3.30
12/22/2009	2.7	16.6	283	1.8	6.9	80.1	33.6	10.1	1.6	0.1	162.0	0.8	4.4	0.2	5.6	-13.9	-3.3	-0.8	3.33
2/18/2010	2.2	13.5	181	4.9	5.9	-53.2	22.1	7.6	1.4	0.1	111.6	3.0	5.4	10.0	3.5	-15.0	-3.0	-2.2	2.91
4/3/2010	1.9	13.9	216	4.0	5.3	45.7	28.2	11.3	1.8	0.1	139.2	2.7	8.8	5.9	25.1	-13.2	-2.1	-2.7	2.49
7/2/2010	ns	ns	ns	ns	ns	ns	ns	ns	ns	ns	ns	ns	ns	ns	ns	ns	ns	ns	ns
7/13/2010	2.4	19.8	79	1.1	6.1	27.5	22.0	6.4	1.3	0.2	96.0	4.3	3.9	0.2	14.6	-14.2	-2.4	-2.0	3.47
10/2/2010	ns	ns	ns	ns	ns	ns	ns	ns	ns	ns	ns	ns	ns	ns	ns	ns	ns	ns	ns
11/24/2010	3.3	19.0	257	3.1	6.7	-11.7	27.2	12.4	2.2	0.1	140.4	5.4	5.8	1.9	26.3	-14.7	-2.5	-1.2	2.19
1/29/2011	ns	ns	ns	ns	ns	ns	ns	ns	ns	ns	ns	ns	ns	ns	ns	ns	ns	ns	ns
4/10/2011	ns	ns	ns	ns	ns	ns	ns	ns	ns	ns	ns	ns	ns	ns	ns	ns	ns	ns	ns
10/20/2011	ns	ns	ns	ns	ns	ns	ns	ns	ns	ns	ns	ns	ns	ns	ns	ns	ns	ns	ns
MW-A																			
9/30/2008	3.5	21.8	955	5.4	6.5	101.4	89.4	35.4	52.0	0.3	453.6	24.0	24.2	67.2	98.6	-11.6	-1.7	-0.5	2.52
1/19/2009	3.2	16.4	849	1.7	6.8	-72.0	85.2	33.5	52.6	0.2	450.0	7.9	23.4	46.8	97.7	-11.1	-2.0	-0.3	2.55
2/27/2009	3.0	15.6	887	4.6	6.7	89.1	67.7	29.7	32.7	0.2	397.2	6.7	22.2	66.1	98.3	-12.2	-1.9	-0.5	2.28
4/24/2009	2.4	16.7	827	3.3	6.3	60.3	88.8	35.7	40.3	0.2	404.4	19.5	20.7	101.1	76.0	-11.1	-1.8	-0.8	2.49
7/31/2009	3.3	20.3	916	2.4	6.3	47.8	96.1	39.8	45.7	0.2	430.8	22.3	21.9	66.2	82.4	-10.9	-1.7	-0.7	2.42
10/9/2009	3.0	21.4	888	3.0	6.2	192.4	81.5	35.3	35.2	0.2	350.4	8.5	16.8	107.3	90.0	-11.3	-1.6	-0.9	2.31
11/1/2009	2.7	20.8	1032	4.9	5.6	196.7	97.7	39.7	33.5	0.3	372.0	9.4	15.7	188.3	73.1	-11.9	-1.6	-1.4	2.46

12/22/2009	2.7	17.2	740	3.0	6.8	124.9	66.1	28.9	35.3	0.2	394.8	5.1	13.9	60.9	83.0	-11.5	-2.0	-0.4	2.28
2/18/2010	2.4	15.4	763	1.7	6.2	-74.6	62.6	30.8	37.4	0.2	411.6	13.0	19.6	42.1	87.4	-12.0	-1.7	-1.0	2.03
4/3/2010	2.2	15.2	898	1.2	6.1	31.1	76.7	33.8	36.0	0.2	346.8	40.8	20.3	117.3	72.5	-11.4	-1.7	-1.2	2.27
7/2/2010	2.6	18.2	1032	1.3	6.7	3.6	85.2	37.8	54.7	0.2	408.0	36.8	34.4	107.1	76.9	-11.7	-2.0	-0.4	2.26
7/12/2010	2.5	19.0	1006	1.1	6.6	10.5	88.0	37.4	55.3	0.2	411.6	33.7	31.4	95.7	44.9	-10.2	-2.2	-0.5	2.35
10/2/2010	3.7	21.1	886	1.5	6.2	83.7	74.9	33.3	57.2	0.2	432.0	16.8	27.3	57.3	60.3	-10.9	-1.8	-0.9	2.25
11/24/2010	3.4	21.2	838	3.4	5.9	12.2	74.0	32.8	54.5	0.3	422.4	9.8	24.0	45.2	84.9	-12.2	-1.6	-1.2	2.26
1/29/2011	3.4	21.7	818	5.3	6.3	6.0	50.5	21.7	32.7	0.3	396.0	7.9	25.2	36.5	86.9	-11.8	-1.7	-1.0	2.33
4/10/2011	3.1	16.8	823	3.7	6.3	25.5	74.8	28.9	37.9	0.2	416.4	6.3	14.9	44.5	75.7	-12.0	-1.8	-0.8	2.59
10/20/2011	3.7	19.9	770	2.5	6.6	49.9	66.1	28.9	35.3	0.2	384.0	6.3	14.9	74.5	59.4	-11.9	-2.0	-0.6	2.28
MW-D																			
9/30/2008	3.4	19.7	1634	0.9	6.8	127.2	126.1	28.9	119.1	0.2	657.6	198.3	49.7	2.2	146.9	-12.0	-1.8	0.1	4.37
1/20/2009	3.2	14.4	1609	2.9	7.4	140.1	110.8	27.4	114.4	0.2	673.2	180.9	48.5	7.6	132.7	-12.4	-2.4	0.6	4.04
2/27/2009	3.0	12.9	1605	3.1	7.2	166.6	126.6	24.3	125.1	0.1	663.6	169.4	48.1	5.3	143.6	-12.5	-2.1	0.4	5.22
4/26/2009	2.5	15.0	1589	2.4	6.7	177.1	84.7	60.5	122.4	0.2	518.4	163.6	47.6	5.2	114.6	-11.9	-1.9	-0.4	1.40
7/31/2009	3.3	18.1	1617	3.2	6.4	142.2	74.3	55.7	127.6	0.2	450.0	188.2	50.6	5.2	112.4	-12.3	-1.6	-0.8	1.33
10/9/2009	3.0	17.4	1456	1.3	6.2	161.9	100.3	48.0	123.0	0.2	633.6	73.0	27.2	6.4	130.2	-12.5	-1.5	-0.7	2.09
11/1/2009	2.7	19.7	1318	6.1	6.7	173.6	96.1	46.2	121.7	0.2	644.4	84.4	58.7	7.5	130.0	-12.3	-1.8	-0.2	2.08
12/22/2009	2.6	15.5	1211	5.5	7.1	-43.9	92.7	44.5	122.3	0.2	655.2	75.0	49.1	8.9	110.3	-12.7	-2.2	0.2	2.08
2/18/2010	2.2	12.9	1326	4.0	6.6	24.4	93.9	45.6	117.7	0.2	644.4	84.4	58.7	7.5	138.7	-12.5	-1.7	-0.4	2.06
4/3/2010	1.9	12.9	2012	2.2	6.4	148.6	123.3	59.3	152.4	0.2	624.0	223.8	107.5	5.9	140.9	-12.6	-1.6	-0.5	2.08
7/2/2010	ns	ns	ns	ns	ns	ns	ns	ns	ns	ns	ns	ns	ns	ns	ns	ns	ns	ns	ns
7/13/2010	2.4	17.4	1602	1.1	6.6	-17.7	103.2	50.0	152.0	0.2	546.0	184.7	74.3	0.1	ns	-13.1	ns	-0.4	2.06
10/2/2010	3.6	18.7	1544	2.9	6.4	49.2	100.9	48.6	152.7	0.3	584.4	162.9	67.7	0.3	78.8	-13.3	-1.8	-0.5	2.08
11/24/2010	3.3	18.8	1512	4.4	6.6	-39.1	103.1	49.6	154.3	0.3	576.0	150.9	61.0	1.2	114.1	-13.8	-1.8	-0.3	2.08
1/29/2011	3.3	15.9	1499	5.2	6.7	125.8	119.9	57.4	162.9	0.5	556.8	147.7	71.8	2.0	87.4	-13.5	-2.0	-0.2	2.09
4/10/2011	3.1	18.0	1501	7.6	6.6	131.1	114.2	57.1	153.7	0.5	622.8	149.1	73.5	3.1	120.9	-14.1	-1.8	-0.2	2.00
10/20/2011	3.7	18.1	1339	3.6	6.8	48.0	100.3	48.0	123.0	0.2	636.0	90.2	67.4	6.8	104.9	-13.9	-1.9	-0.1	2.09
MW-C																			
9/30/2008	3.5	19.4	1344	7.1	6.4	78.6	104.0	62.9	87.5	0.5	427.2	81.3	31.8	214.0	92.4	-13.2	-1.7	-0.6	1.65
1/19/2009	3.2	13.8	1116	2.2	6.9	74.9	76.3	49.3	84.6	0.3	439.2	37.3	36.5	128.0	85.2	-11.6	-2.1	-0.3	1.55
2/27/2009	3.0	13.6	1052	1.7	7.0	79.8	49.2	36.9	71.3	0.3	454.8	28.0	36.4	104.7	84.9	-11.8	-2.2	-0.4	1.33
4/24/2009	2.3	15.5	1133	3.6	6.6	-10.9	75.9	59.8	88.9	0.5	542.4	49.3	59.6	25.9	96.1	-15.1	-1.9	-0.4	1.27
7/31/2009	3.3	18.0	1016	4.3	6.5	50.2	55.8	41.3	78.8	0.3	414.0	30.6	31.3	76.7	80.4	-12.7	-1.9	-0.8	1.35
10/9/2009	3.0	17.9	843	1.6	7.0	12.0	55.4	38.3	70.3	0.3	356.4	14.3	19.9	49.9	84.8	-11.1	-2.2	-0.3	1.45
11/1/2009	2.7	18.1	1174	4.8	6.7	76.6	63.3	45.6	78.1	0.4	500.4	29.5	30.8	23.1	113.2	-14.5	-1.9	-0.4	1.39
12/22/2009	2.6	14.4	1581	4.3	6.9	-131.3	80.9	73.8	125.0	0.4	793.2	68.6	62.8	27.1	170.7	-16.1	-1.8	-0.1	1.10
2/18/2010	2.3	13.4	1424	2.2	6.3	83.3	82.0	63.5	100.6	0.3	728.4	48.5	45.2	32.8	171.9	-15.7	-1.5	-0.7	1.29
4/3/2010	2.0	12.5	1153	2.3	6.1	-28.5	76.2	58.7	92.0	0.4	592.8	33.4	45.6	19.4	157.7	ns	-1.5	-0.9	1.30
7/2/2010	2.6	15.9	1154	1.3	6.7	1.7	71.6	52.0	90.2	0.3	554.4	48.5	49.9	39.5	97.8	-15.8	-1.9	-0.4	1.38
7/12/2010	2.5	16.5	1136	1.2	6.7	13.2	68.5	52.9	90.5	0.3	514.8	44.0	45.7	40.5	88.2	-14.5	-1.9	-0.5	1.30
10/2/2010	3.6	18.0	1009	1.4	5.6	29.1	53.5	41.2	76.8	0.3	408.0	27.7	27.5	87.4	59.2	-13.6	-1.7	-1.7	1.30
11/27/2010	3.4	18.6	931	3.4	6.2	10.7	53.6	40.9	76.6	0.4	411.6	24.4	26.1	80.4	74.5	-12.9	-1.7	-1.1	1.31
1/29/2011	3.3	16.2	901	2.8	6.1	11.8	35.2	26.4	44.1	0.3	378.0	23.4	31.2	66.9	ns	ns	ns	-1.4	1.33
4/10/2011	3.1	15.0	825	4.2	6.3	29.4	33.6	26.1	41.2	0.2	398.4	24.9	28.5	48.3	81.9	-12.4	-1.8	-1.2	1.29
10/20/2011	3.5	17.3	833	5.4	6.7	-107.1	60.2	37.4	57.1	0.7	418.8	34.9	38.5	71.4	74.1	-14.0	-2.0	-0.5	1.61

DO = dissolved oxygen, ORP = oxidation reduction potential, DIC = dissolved inorganic carbon, $\delta^{13}C$ from dissolved inorganic carbon, pCO_2 = partial pressure of CO_2, Si_{Ca} = the saturation index with respect to calcite.

VITA

Christopher J. Geyer

Candidate for the Degree of

Master of Science

Thesis: Steep spatial chemical gradients in shallow groundwater contaminated with nitrate at a residential site

Major Field: Geology

Biographical:

Education:

- Completed the requirements for the Master of Science in Geology at Oklahoma State University, Stillwater, Oklahoma in May, 2014.
- Completed the requirements for the Bachelor of Science in Geology at Oklahoma State University, Stillwater, Oklahoma in 2011.

Experience:

- National Science Foundation Research -International research in Botswana, Africa; summer 2010; Oklahoma State University, Stillwater, OK
- Geochemistry laboratory technician; fall 2010 – spring 2014; Oklahoma State University, Stillwater, OK
- Rapid response research of the Deepwater Horizon spill; spring 2011; Oklahoma State University, Stillwater, OK
- Teaching Assistant – Field Camp; summer 2013; Oklahoma State University, Stillwater, OK

Publications:

- Geyer, C. Paizis, N., Atekwana, E. 2012. Temporal investigation of the sources and fate of nitrate contamination at a residential site. Geological Society of America Abstracts with Programs. Vol. 44, No. 7, p.393.
- Paizis, N., Geyer, C., Kgaodi, O., Koontse, T., Akoko, E., Cruse, A.M., Atekwana, E.A., Molwalefhe, L., Masamba, W., Ringrose, S., 2010. Of cows, hippos and carbon: Conducting international research with U.S. and Botswanan undergraduate and graduate students in the Okavango Delta. Geological Society of America Abstracts with Programs, Vol. 42, No. 5, p. 438.
- Geyer, C., Paizis, N., Kgaodi, O., Koontse, T., Akoko, E., Atekwana, E.A., Cruse, A.M., Molwalefhe, L., Masamba, W., Ringrose, S., 2010. The effects of evaporation on the chemistry of the Okavango River, northwestern Botswana. Geological Society of America Abstracts with Programs, Vol. 42, No. 5, p. 292.